CHAPTER 8

Photometry and Colorimetry of Planets and Satellites

By DANIEL L. HARRIS
*Yerkes Observatory**

1. INTRODUCTION

THE photometry of the planets and the satellites has been the subject of many investigations, both observational and theoretical. As good summaries of the earlier work are available in the *Handbuch der Astrophysik*, Volumes **2** and **7** (Berlin, 1929, 1936), we restrict the present discussion to the more recent observational and theoretical results, except where earlier data are needed for the treatment of specific problems. However, frequent reference will be made to Zöllner's (1865) excellent magnitude observations of the sun, moon, and planets made from 1862 to 1864 and to Müller's (1893) comprehensive investigations made from 1877 to 1891. These are of particular importance in connection with the possibility of long-period variations in the magnitudes of the planets.

For the purposes of this chapter, systematic observations of magnitudes and colors of planets and satellites have been made with the 82-inch telescope of the McDonald Observatory since 1950. These observations, here included in summary form, were made by Dr. Kuiper and the writer. We wish to acknowledge the assistance received from the Office of Naval Research, which supported the initial phases of this work under Contract No. N9onr-87100, starting July 1, 1950, under the title "The Determination of Photometric Constants of the Solar System."

2. STANDARD SYSTEM OF MAGNITUDES AND COLORS

As in most photometric investigations, it is desirable to reduce all the observations to a standard system so that the various results may be

* Now at T.E.N.S. Corporation, Bethesda, Md.

directly compared. In the present discussion we have adopted the U, B, V color system of Johnson and Morgan (1953) and the R, I color system of Hardie (1956).

The V (visual) magnitude has for solar radiation an effective wave length of about 0.554μ, which is very close to that of the average eye for the higher intensities. The zero point of the V magnitudes was fixed to obtain agreement with the IPv magnitudes of the North Polar Sequence.

The effective wave lengths for solar radiation of the U (ultraviolet), B (blue), V (visual), R (red), and I (infrared) magnitudes are given in Table 1. The zero points of the U and B magnitudes were so chosen that the colors $U - B$ and $B - V$ are 0.00 for unreddened stars of spectral type A0 V on the MK system of spectral classification (Johnson and Morgan, 1953). However, as all discussion of colors in this chapter is with reference to the sun, we can consider the zero points of the colors to be defined by

TABLE 1

EFFECTIVE WAVE LENGTHS OF PHOTOELECTRIC MAGNITUDES FOR SOLAR RADIATION

	U	B	V	R	I
$\lambda(\mu)$	0.353	0.448	0.554	0.690	0.820
$\lambda^{-1}(\mu)$	2.83	2.23	1.81	1.45	1.22

the mean values for stars of the same spectral type, G2 V, i.e., $U - B = 0.14$, $B - V = 0.63$, $V - R = 0.45$, and $R - I = 0.29$.

The choice of the V magnitude system was made because the important earlier observations were made visually. In future investigations the use of a magnitude with a shorter effective wave length would admit more accurate intercomparison of the major planets, in which the visual region is strongly affected by their atmospheric bands (e.g., Hardie and Giclas, 1955).

The relative response to solar radiation of the 1P21 photomultiplier and filter combinations used in establishing the U, B, V system (Johnson and Morgan, 1951) is shown in Figure 1. The plotted points include the effects of one air mass of extinction, two reflections by aluminized mirrors, and the solar absorption lines averaged over intervals of 100 A. The integrated effects of the absorption lines amount to about 0.66 mag. for U, 0.29 mag. for B, and 0.07 mag. for V.

Table 2 gives the V magnitudes and $B - V, U - B$ colors for a few of the bright stars employed by earlier investigators in their photometric work. These results have been compiled from published photoelectric

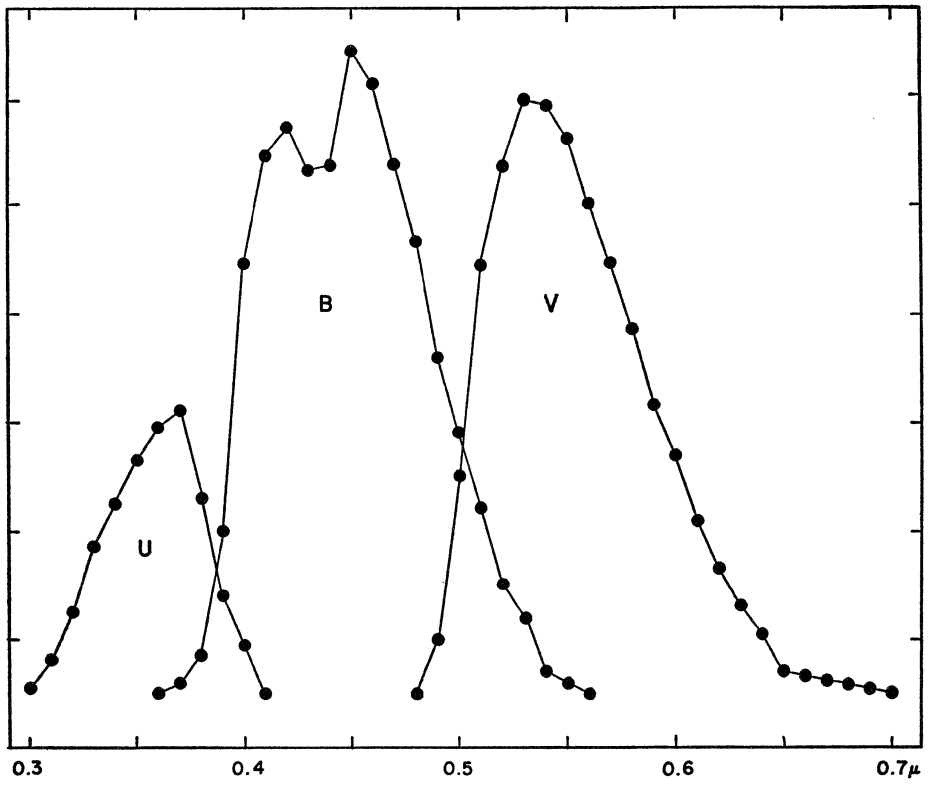

FIG. 1.—Relative wave-length response of photometric system to solar radiation. See alsc Table 1.

TABLE 2

MAGNITUDES AND COLORS OF COMPARISON STARS FOR SUN AND PLANETS

Star	V	$B-V$	$U-B$	MK
α CMa.....	$-1^m.42$	$+0^m.01$	$-0^m.08$	A1 V
α Boo.....	−0.06	+1.23	+1.26	K2p III
α Lyr.....	+0.04	0.00	−0.01	A0 V
α Aur.....	+0.05	+0.80	+0.44	G8 III:+F
β Ori.....	+0.14v*	−0.04	−0.67	B8 Ia
α CMi.....	+0.37	+0.41	0.00	F5 IV-V
α Aql.....	+0.77	+0.22	+0.08	A7 IV, V
α Tau.....	+0.86v†	+1.53	+1.89	K5 III
β Gem.....	+1.16	+1.02	+0.84	K0 III
α Cyg.....	+1.26	+0.09	−0.25	A2 Ia
α Leo.....	+1.36	−0.11	−0.36	B7 V
α Gem AB.....	+1.60	+0.02	0.00	Al V+A5 m
α Ari.....	+2.00	+1.15	+1.12	K2 III

* Variable; range 0.12 mag.
† Range 0.15 mag.

measures and from unpublished observations made at the McDonald and Lowell Observatories.

3. THE SUN

A determination of the albedos of the planets and satellites requires a knowledge of the apparent magnitude of the sun. Since Kuiper's (1938) discussion, three new determinations of the magnitude of the sun have been made, and the earlier visual data can be improved by a redetermination of the magnitudes of the comparison stars.

The visual determinations of the magnitude of the sun are those given by Russell (1916*a*) and Kuiper (1938). They are reduced to the V system in Table 3. Giving half-weight to Pickering's determination, which is of lower internal accuracy, we have, from the visual determinations, $V = -26.88$.

Woolley and Gascoigne (1948) have made a spectrophotometric determination of the difference in magnitude between the sun and Sirius, which

TABLE 3

VISUAL DETERMINATIONS OF MAGNITUDE OF SUN

Observer	V	Observer	V
Zöllner.....	−26.82	Ceraski....	−26.87
Fabry.....	−26.90	Pickering...	−26.98

gives $V = -26.99$ for the sun. However, this is essentially a monochromatic magnitude, in that it does not include the effects of absorption lines in either the sun or Sirius. For the sun the effect amounts to 0.073 mag. (see Sec. 2), while for Sirius the effect is only about 0.01 mag. (e.g., Milford, 1950). Allowing for this difference, we obtain $V = -26.93$.

Nikonova (1949) made a photoelectric determination of the magnitude of the sun, using the moon as an intermediary. Her result appears to be quite reliable and gives $V = -26.80$.

Stebbins and Kron (1956) have recently made a determination of the magnitude of the sun, using a standard lamp as an intermediary. They conclude that $V = -26.73$, with an internal probable error of less than 0.02 mag.

Comparing the three recent determinations, which are of comparable internal accuracy, we see that the systematic errors affecting one or more of the values are far more important than the accidental errors of observation. If we give equal weight to the three modern determinations and to the mean of the visual determinations, we find $V = -26.83$. Double weight for the photoelectric determinations gives $V = -26.81$, which we have adopted.

We have omitted here the two photographic determinations by King and Birke and the radiometric determination by Pettit and Nicholson used by Kuiper (1938) in his discussion, because of uncertainties in the reduction to the V system.

We have not assigned a mean error to the magnitude of the sun, as it depends on the relative weights assigned to the individual determinations. However, the adopted value is uncertain by not more than ± 0.1 mag.

4. MAGNITUDES OF THE PLANETS

4.1. Introduction

The apparent magnitude of a planet is a function of the planet's distance from the sun, r, the planet's distance from the earth, d, and the solar phase angle, α, which is the angular distance at the planet between the earth and the sun. For Mercury, Venus, and the moon the solar phase angle varies from 0° to 180°; for Mars the angle can attain a value of about 47°, while for the more distant planets the angle reaches only a few degrees.

Neglecting possible variations in brightness due to rotation or intrinsic causes, the observed magnitude of a planet is given by

$$V = V(1, 0) + 5 \log rd + \Delta m(\alpha), \qquad (1)$$

where $V(1, 0)$ is the magnitude of the planet reduced to unit distance from the sun and earth and phase angle zero and $\Delta m(\alpha)$ is the correction for the variation in magnitude of the planet with phase angle.

The quantity $\Delta m(\alpha)$ is composed of two parts; the first arises from the fact that the fraction of the illuminated disk visible from the earth varies with α, while the second, and much larger, effect is due to the properties of diffuse reflection from the planet's surface or atmosphere.

From the observational point of view, it is sufficient to express $\Delta m(\alpha)$ as a power series in α, retaining as many terms as are required adequately to represent the observations. For the outer planets it is generally sufficient to consider only the first term, and the coefficient of α so found is often referred to as the *phase coefficient.*

The magnitude, $V(1, 0)$, corresponds to the quantity g introduced by earlier investigators; the new symbol is used here to specify the spectral region to which the observations refer.

For some purposes it is convenient to use the *mean opposition magnitude*, V_0, which is related to $V(1, 0)$ by

$$V_0 = V(1, 0) + 5 \log a(a - 1), \qquad (2)$$

where a is the semimajor axis of the planet's orbit.

If the brightness of the planet is *variable*, the problem of predicting the

apparent magnitude at a given time is considerably more complicated. The variability may arise from the following causes: (*a*) the planet's surface is spotted, giving rise to a brightness variation with the rotation period; (*b*) changes in the planet's atmosphere or surface features, giving rise to variations of an irregular character. These may be short-lived or persist for considerable periods of time.

For planets exhibiting intrinsic variability we have tried to determine mean values of $V(1, 0)$ and $\Delta m(\alpha)$ and indicate graphically the variations from these mean values. In particular, it is noted that the variation with rotational phase is a function of solar phase angle as well. This follows not only from geometrical considerations but also because the properties of diffuse reflection must depend on the surface features.

In connection with the question of long-period variations in the magnitudes of the planets, as discussed by Becker (1933, 1948), it is necessary to utilize earlier observations along with the modern photoelectric determinations. Of the older observations, those of Zöllner (1865) and Müller (1893) are considered the most reliable, and we have reduced these results, using modern values of V for the comparison stars and modern phase functions. Because of the uncertainty in the magnitude scales and in the reductions to the standard system, we have omitted all photographic values, except the photovisual determinations by King (1923, 1930), which are considered systematically reliable.

As far as short-period variations are concerned, we have given most of the weight to the photoelectrical results because of their far greater precision.

4.2. Magnitudes of Individual Planets

4.21. *Mercury.*—The variation of Mercury with solar phase angle has been determined by Danjon (1949) over the range $3° < \alpha < 123°$. As the rotation period is equal to the planet's period of revolution around the sun, only small changes from the mean curve are observed at different librations. The corrected analytical expression for the phase function is (Danjon, 1954)

$$\Delta m\,(\alpha) = 3.80\left(\frac{\alpha}{100°}\right) - 2.73\left(\frac{\alpha}{100°}\right)^2 + 2.00\left(\frac{\alpha}{100°}\right)^3. \qquad (3)$$

Danjon's magnitude of Mercury at unit distance is $m_0 = -0.21$. This value may be reduced to the V system by means of an average correction determined from the comparison stars used by Danjon. This gives $V(1, 0) = -0.36$. Danjon also reduced Müller's observations, made in 1878–1888, to his own photometric system and to opposition with the aid of his own $\Delta m(\alpha)$-curve; the result is a value 0.10 mag. brighter, i.e., $V(1, 0) =$

-0.46. As Mercury has no appreciable atmosphere, no long-period variations in the brightness are expected.

4.22. *Venus.*—The variation of Venus with solar phase angle has been determined by Danjon (1949) over the range $0^\circ.9 < \alpha < 170^\circ.7$. His analytical expression for the phase function is

$$\Delta m\,(\alpha) = 0.09\left(\frac{\alpha}{100^\circ}\right) + 2.39\left(\frac{\alpha}{100^\circ}\right)^2 - 0.65\left(\frac{\alpha}{100^\circ}\right)^3. \qquad (4)$$

Danjon's magnitude of Venus, reduced to the V system as was done for Mercury, gives $V(1, 0) = -4.29$. Danjon's reduction of Zöllner's observations made in 1865 gives -4.28, while his reduction of Müller's observations between 1877 and 1890 gives -4.21. These older observations, while of lower weight, give no indication of a long-period variation in the brightness of Venus.

4.23. *The earth.*—The problem of the photometry of the earth has been considered by Danjon in Volume **2**, chapter 15. The analytical phase function was found to be

$$\Delta m\,(\alpha) = 1.30\left(\frac{\alpha}{100^\circ}\right) + 0.19\left(\frac{\alpha}{100^\circ}\right)^2 + 0.48\left(\frac{\alpha}{100^\circ}\right)^3. \qquad (5)$$

The magnitude difference, earth — sun, is 22.94 and shows an annual variation with a range of 0.51. With our adopted magnitude of the sun, -26.81, we obtain $\bar{V}(1, 0) = -3.87$.

As Danjon emphasizes (Vol. **2**, chap. 15, Sec. 3), these results are based on measures of the earth light obtained in France and do not necessarily apply to the earth as a whole. The magnitude of the earth, as seen from the sun, probably shows a diurnal variation due to land and oceans, as well as variations from the variable cloud coverage.

4.24. *Mars.*—The variation in the brightness of Mars with rotational period was first established by Guthnick and Prager (1918) and was recently confirmed by Johnson and Gardiner (1955) and by Kuiper and Harris. The variation is best defined by series of observations made near quadrature. Figure 2, *a*, shows the difference in red magnitude between Mars and β Geminorum observed by Guthnick and Prager in 1916, plotted against the longitude of the central meridian, λ. The 1954 observations of $\bar{V}(1, 0)$ made at the Lowell and McDonald Observatories, when the solar phase angles were greater than 30°, are shown in Figure 2, *b*, while the corresponding $B - V$ colors are shown in Figure 2, *c*. Three observations made at McDonald in 1952 are plotted as open circles.

As was shown by Johnson and Gardiner, the similarity in the variation of V and $B - V$ indicates that the change in blue and ultraviolet light is

considerably less than in visual or red light. This must be largely due to the fact that the Martian atmosphere is nearly opaque to ultraviolet and blue light, where the disk of the planet shows little contrast with rotational phase, while in visual light the atmosphere is more transparent and the contrast of the surface gives rise to the rotational variation observed.

Johnson and Gardiner noted that the scatter of their observations about a mean curve was more than could be explained by observational errors.

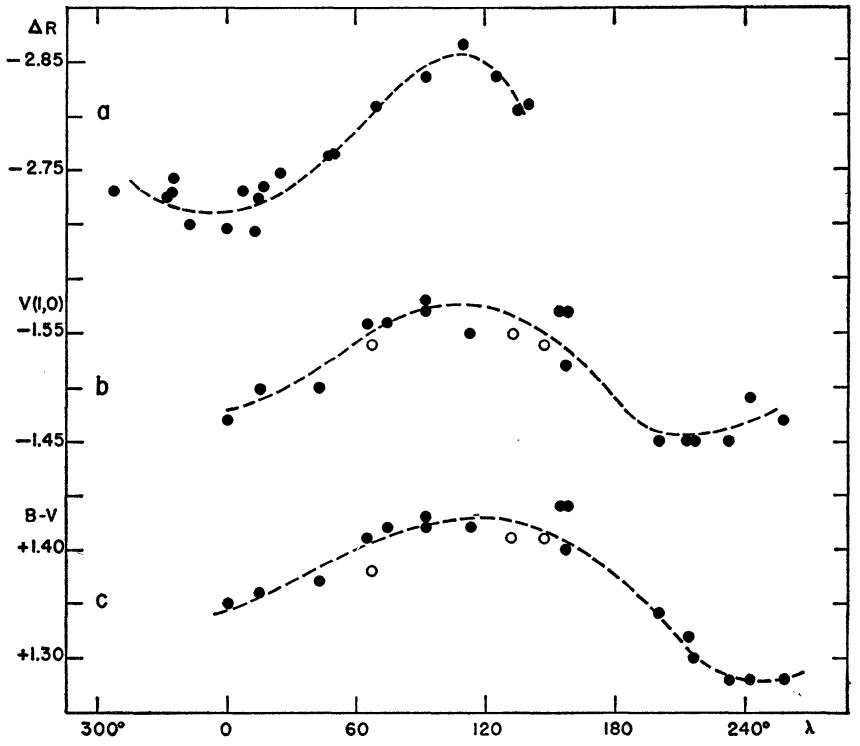

FIG. 2.—Variation of Mars with rotational phase angle. (*a*) In red light (Mars — β Gem) by Guthnick and Prager (1916); (*b*) in yellow light, V (1, 0), from Lowell and McDonald observations (1954); (*c*) in the $B - V$ color. (See text.)

It is probable that variations in the transparency of the Martian atmosphere contributed to this scatter; if the atmosphere is clearer than normal, the observed magnitude will be fainter than average, while an increase in the "haze" will make the observed magnitudes brighter. An extreme example occurred on May 3–4, 1952, when the ultraviolet magnitude of Mars was 0.3 mag. brighter, the blue magnitude about 0.2 mag. brighter, and the visual magnitude 0.1 mag. brighter than average (see Sec. 6.2).

The problem of determining the solar phase variation over the 47° range in phase angle is complicated by the rotational variation and the

changes in the Martian atmosphere; a linear relation satisfies the observations quite well. The extensive photoelectric series at the Lowell Observatory in 1954 gives a phase coefficient of 0.016 mag/degree in the visual region, and 0.017 mag/degree in the blue and ultraviolet. The long series of visual observations by Müller gave 0.015 mag/degree.

Becker (1933) suggested that the mean opposition magnitude of Mars varied with a range of about 0.48 mag., but no period was established. The older measures reduced to the V system are given in Table 4, where it is seen that the values are remarkably accordant and show no evidence of a long-period variation. The mean value of $V(1, 0)$ is -1.52 mag. The reduction to mean opposition is -0.49 mag., giving $\bar{V}_0 = -2.01$.

TABLE 4

VALUES OF V(1, 0) FOR MARS

Opposition	Observer	$V(1, 0)$	Opposition	Observer	$V(1, 0)$
1864–1865...	Zöllner	−1.59	1916.....	King, Pv	−1.52
			1918.....	King, Pv	−1.51
1877–1878...	Müller	−1.44	1920–1921...	King, Pv	−1.45
1879–1880...	Müller	−1.48	1922.....	King, Pv	−1.56
1881–1882...	Müller	−1.57			
1883–1884...	Müller	−1.55	1952.....	Kuiper,	
1886.....	Müller	−1.51		Harris	−1.56
1888–1889...	Müller	−1.52	1954.....	Lowell Obs.	−1.51

4.25. *Jupiter.*—Accurate photometric data for Jupiter are quite limited, and it is not possible to give a completely satisfactory description of its brightness variations. Guthnick and Prager (1918) found no evidence for a variation with rotational phase during the opposition of 1917–1918, but during the 1920 opposition Guthnick (1920) found a variation of 0.14 mag.

A similar situation obtains with regard to variation with solar phase angle. Müller's extensive visual observations indicate a small value for the phase coefficient, of the order of 0.005 mag/degree, and a similar small variation is indicated by Güssow's (1929) observations of 1928. On the other hand, the observations at the 1917 opposition by Guthnick and Prager gave a well-determined variation amounting to 0.015 mag/degree, while the opposition of 1918–1919 gave a value about half as large (reported by Schönberg, 1921). Figure 3, *a*, *b*, and *c*, illustrates the phase differences found by Müller, by Güssow, and by Guthnick and Prager in 1917. It is seen that the slope fitting the 1917 results is not supported by the other observations. The phase coefficient may be variable; but from

theoretical considerations the smaller value of 0.005 mag/degree appears more representative than the larger value (see Sec. 8.6).

Becker (1933) found the mean opposition magnitudes of Jupiter to vary with an amplitude of 0.34 mag. in a period of 11.6 ± 0.4 years. We have reduced the older observation to the V system in Table 5 and plotted them in Figure 4. The mean for 23 oppositions is $V(1, 0) = -9.25$, with the individual oppositions varying from −9.03 to −9.48, a range of 0.45. As the same observers' values for Mars and Saturn show, at most, very small variations, it is concluded that the larger changes found for Jupiter are real. The data in Table 5 are not sufficient to establish a period, but the variation may well be correlated with changes on the surface features, as

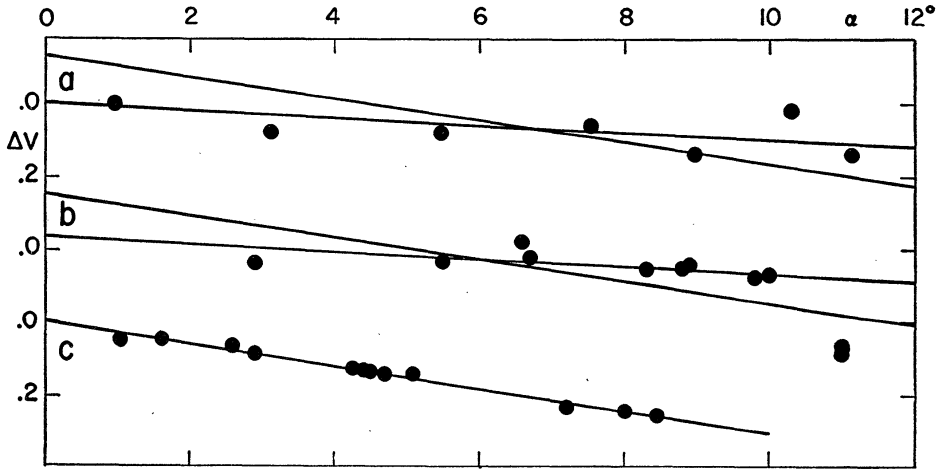

FIG. 3.—Variation of Jupiter with solar phase angle. (*a*) Visual means from Müller; (*b*) photoelectric observations by Güssow (1928); (*c*) photoelectric observations by Guthnick and Prager (1917).

TABLE 5

VALUES OF $V(1, 0)$ FOR JUPITER

Opposition	Observer	$V(1, 0)$	Opposition	Observer	$V(1, 0)$
1862.....	Zöllner	−9.22	1889.....	Müller	−9.09
1863.....	Zöllner	−9.22	1890.....	Müller	−9.07
1864.....	Zöllner	−9.34			
			1915.....	King, Pv	−9.39
1878.....	Müller	−9.03	1916.....	King, Pv	−9.18
1879–1880...	Müller	−9.14	1918.....	King, Pv	−9.16
1880–1881...	Müller	−9.19	1920.....	King, Pv	−9.24
1881–1882...	Müller	−9.28	1921.....	King, Pv	−9.41
1883.....	Müller	−9.24	1922.....	King, Pv	−9.30
1883–1884...	Müller	−9.28			
1885.....	Müller	−9.25	1951.....	Kuiper	−9.46
1886.....	Müller	−9.18	1952.....	and	−9.48
1887.....	Müller	−9.11	1954.....	Harris	−9.39

Becker (1933) suspects. The reduction to mean opposition is −6.70 mag.; therefore, $\bar{V}_0 = -2.55$ (var.).

4.26. *Saturn.*—The presence of the Rings makes the study of Saturn's disk very difficult, but the brightness of the total light is surprisingly well known. In regard to a variation with rotational phase, the results of Guthnick and Prager (1918) indicated that the system did not vary more than ±0.01 mag. at the oppositions of 1914–1915 and 1917.

The variation in the magnitude of the Saturn system with solar phase angle is nearly linear over the observable range of 6°, and the phase coefficient, according to Müller, is 0.044 mag/degree. Guthnick and Prager's

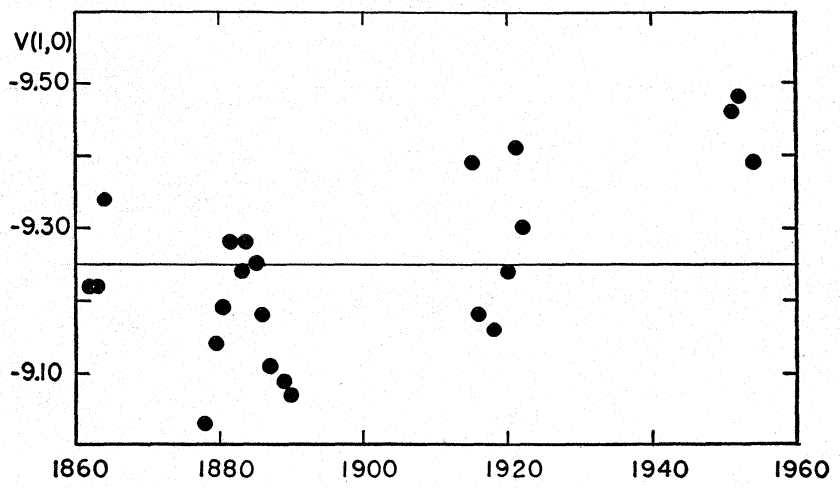

FIG. 4.—Long-period variation of Jupiter (see Table 5)

observations in 1914–1915 and 1917 give a somewhat smaller value, about 0.033 mag/degree, while Guthnick's observations in 1918 and 1920 (quoted by Schönberg, 1921) give 0.043 mag. and 0.049 mag/degree. The phase coefficient, therefore, seems to vary slightly with the inclination of the Rings and, hence, the fraction of the total light they contribute. It should be mentioned that Guthnick's (1918) observations, made very close to opposition, are nearly 0.15 mag. brighter than would be expected from the linear formula; however, the observation on January 8, 1918, with $\alpha = 2^\circ.60$, is also discordant, so that this brightening near opposition must be confirmed before the linear phase function is abandoned.

The foregoing discussion applies to the combined light of the system; the phase correction for the ball of the planet alone is undoubtedly much smaller (Schönberg, 1921) and is probably of the order of 0.01 mag/degree or less.

The magnitude of the system varies greatly with changing aspect of the Rings. Müller's empirical formula to reduce the brightness to "no-ring" is

$$\Delta V = +2.60 \sin B - 1.25 (\sin B)^2 \qquad (6)$$

where B is the saturnicentric latitude of the earth. The quantity ΔV was determined from observations made between 1877 and 1891, when the earth was south of the planet's equatorial plane. Becker (1948) suggests that the correction depends on whether the earth is north or south of the plane, a suggestion that should be tested by observations during the coming oppositions.

Becker (1948) finds that the mean opposition magnitude of the planet, reduced to "no-ring," varies irregularly by 0.33 mag. The results of our reduction of the older measures are given in Table 6. It is seen that the

TABLE 6

VALUES OF $V(1, 0)$ FOR SATURN (NO-RING)

Opposition	Observer	$V(1, 0)$	Opposition	Observer	$V(1, 0)$
1862.....	Zöllner	−8.84	1883–1884...	Müller	−8.87
1863.....	Zöllner	−8.82	1884–1885...	Müller	−8.86
			1885–1886...	Müller	−8.92
1877–1878...	Müller	−8.86	1886–1887	Müller	−8.88
1878.....	Müller	−8.88	1887–1888...	Müller	−8.87
1879–1880...	Müller	−8.87	1891.....	Müller	−8.94
1880–1881...	Müller	−8.90			
1881–1882...	Müller	−8.89	1951.....	Kuiper,	−8.87
1882–1883...	Müller	−8.89	1952.....	Harris	−8.86

values of $V(1, 0)$ show very little scatter, from −8.94 to −8.82 mag. only, while Müller's observations from 1877 to 1891 show a total range of only 0.08 mag. It appears that the brightness of the planet is remarkably constant, the mean value being $V(1, 0) = -8.88$. The reduction to mean opposition is +9.55 mag., so that $V_0 = +0.67$.

4.27. *Uranus.*—The question as to whether Uranus varies in light with its rotation period of 10.84 hours (Lowell and Slipher, 1912; Moore and Menzel, 1930) is difficult to decide. To show such a variation, the surface of the planet must develop temporary spots, and the planocentric latitude of the earth must be small. Such conditions may have been satisfied in 1917, when Campbell (1917, 1936) found Uranus to vary by 0.15 mag. in a period of 10^h49^m, and during the interval from 1920 to 1930, when several visual and photographic series (Becker, 1928; Slavinas, 1928; Goddard, 1930) indicated variations with the same period and amplitudes ranging from 0.03 to 0.15 mag.

On the other hand, photoelectric observations by Stebbins and Jacobsen (1928), Güssow (1929), Calder (1936), Hardie and Giclas (1955), and Kuiper and Harris, at the oppositions of 1927, 1928, 1934–1935, 1935–1936, and from 1950 to 1955, respectively, show no indications of a variation in brightness with rotational phase, in spite of the much higher accuracy of these observations. Until the rotational variation has been confirmed by high-precision photoelectric series, it is probably best to use the period of rotation as determined spectroscopically.

The solar phase angle of Uranus attains only 3°, but Stebbins and Jacobsen (1928) found a phase coefficient of 0.0028 mag/degree. The Lowell observers find a somewhat smaller value, of the order of 0.001 mag/degree.

TABLE 7

VALUES OF $V(1, 0)$ FOR URANUS

Opposition	Observer	$V(1, 0)$	Opposition	Observer	$V(1, 0)$
1864.....	Zöllner	−7.19	1928.....	Güssow	−7.20
1878.....	Müller	−6.90	1935.....	Calder	−7.26
1879.....	Müller	−7.06	1936	Calder	−7.27
1880.....	Müller	−7.12			
1881.....	Müller	−7.13	1949–1950...	Lowell Obs.	−7.19
1884.....	Müller	−7.14	1950–1951...	Lowell Obs.	−7.20
1885.....	Müller	−7.08	1951–1952...	Lowell Obs.	−7.19
1886.....	Müller	−7.00			
1888.....	Müller	−7.01	1952.....	Kuiper, Harris	−7.18
1927.....	Stebbins and Jacobsen	−7.16	1953–1954...	Lowell Obs.	−7.17

Becker's investigation (1948) of the mean opposition magnitude of Uranus would indicate that Uranus varies 0.29 mag. with a period of the order of 8 years, superposed on a variation of 0.26 mag. with a period of 82 years. The latter variation, interpreted as the effect of the oblateness of the planet, gives too large a value of the polar compression.

As far as the 8-year variation is concerned (which seems to have found some confirmation, Ashbrook, 1948), the observations at the Lowell Observatory from 1949 to 1955, already mentioned, which cover more than half the suspected period, show no evidence for a variation larger than about 0.01 mag., which may well be due to unavoidable uncertainties.

The results of our reduction of the older series of measures is given in Table 7. It is seen that Müller's observations show considerable scatter. The mean of his 92 observations is 0.12 mag. fainter than our adopted value of $V(1, 0) = 7.19$, while Calder's observations are about 0.08 mag.

brighter than our adopted value. As Hardie and Giclas (1955) have emphasized, the strong absorption bands in the visual region make the reductions of one series to another rather uncertain. The reduction to mean opposition is +12.71 mag. or $\bar{V}_0 = +5.52$.

4.28. *Neptune.*—The rotation period of Neptune determined spectroscopically by Moore and Menzel (1928) is 15.8 ± 1 hours. A number of photographic and visual investigations of Neptune have indicated periodic variations in brightness which were attributed to rotation. However, as in the case of Uranus, the photoelectric observations fail to show any evidence of variation (Calder, 1938; Hardie and Giclas, 1955; and this chapter). To indicate the attainable accuracy of photoelectric observations as applied to the possible short-period variation of Neptune, we find from Hardie's (1953) observations on 15 nights from June 10 to July 3, 1953,

TABLE 8

VALUES OF $V(1, 0)$ FOR NEPTUNE

Opposition	Observer	$V(1, 0)$	Opposition	Observer	$V(1, 0)$
1864.....	Zöllner	−6.77	1886–1887...	Müller	−6.89
1878.....	Müller	−7.01	1949–1950...	Lowell Obs.	−6.79
1881–1882....	Müller	−6.96	1950–1951...	Lowell Obs.	−6.83
1883.....	Müller	−6.87	1951–1952...	Lowell Obs.	−6.83
1883.....	Müller	−6.97	1951–1952...	Kuiper	−6.87
1884–1885....	Müller	−6.89	1952–1953...	and	−6.84
1885–1886....	Müller	−6.82	1953–1954...	Harris	−6.85

that two nights deviated by 0.006 mag. from the mean, two nights show deviations of 0.005 and 0.004 mag., while the remaining eleven nights deviate by 0.002 mag. or less. It should be remembered that these deviations also include possible variations in the brightness of the comparison star. As, furthermore, the announced variations do not agree with the spectroscopically determined period or with each other, the reality of these results is in doubt.

The period of rotation of a planet determined spectroscopically is independent of the assumed value of the planet's diameter (Moore and Menzel, 1930); recent suggestions that the period found by Menzel and Moore should be shortened because of Kuiper's (1949) new value for the apparent diameter of the planet are, therefore, incorrect.

The observed range in phase angle is very small, and no variation due to it has been observed. Becker (1933) suggested that the mean opposition magnitudes of Neptune showed a variation of 0.36 mag. in a period of 21 ± 0.6 years. Our reduction of the older measures are given in Table 8.

We find that the mean of thirteen oppositions gives $V(1, 0) = -6.87$, with a range of individual values of 0.24 mag. Most of this scatter is probably due to observational error and difficulties of reduction to the standard system. The difference between the Lowell and McDonald results in 1951–1952, for example, can be attributed to the heavy methane bands of Neptune and the slight difference in filter-cell combination employed at the two observatories. The reduction to mean opposition is +14.71 mag., so that $\bar{V}_0 = +7.84$.

4.29. *Pluto.*—Observations of Pluto made by Walker and Hardie (1955) in 1954 and 1955 combined with earlier observations by Kuiper made in 1952 and 1953 show that Pluto varies in light by about 0.11 mag. in a period of 6.390 ± 0.003 days. A plot of the observations is given in Figure

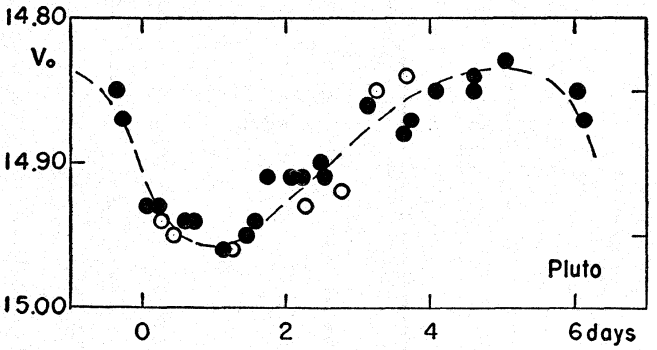

FIG. 5.—Variation of Pluto with rotational phase. *Open circles:* observations by Kuiper (1952 and 1953); *filled circles:* observations by Walker and Hardie (1954 and 1955).

5, where the open circles refer to the 1952–1953 observations by Kuiper. This variation is assumed to be due to the rotation of the planet; the significance of such a long period of rotation has been discussed by Kuiper (1953, 1956*a*).

Any variation over the small range of solar phase angle, ~1°.5, would be difficult to establish because of the much larger rotational variation.

The mean opposition magnitude of $V_0 = 14.90$, and the reduction to mean opposition is +15.91 mag., so that $V(1, 0) = -1.01$.

4.3 Summary of the Photometric Data on the Planets

The values of the magnitudes at unit distance from the earth and sun, $V(1, 0)$, the corresponding magnitudes at mean opposition, and remarks concerning the variability of the brightness of the planets are summarized in Table 9. Observations of the solar constant by the Astrophysical Observatory of the Smithsonian Institution suggest that the solar radiation may vary by as much as ±1.5 per cent over long periods, with short-

period variations of the order of ±0.4 per cent. Such variations are too small to be established by direct observation of the magnitude of the sun. However, as any change in the brightness in the sun would be noted in the reflected light from the planets, satellites, and asteroids, a number of investigations have been made to check the constancy of the sun's radiation by observations of the planets.

Uranus and Neptune appear to be most suitable for this purpose, and observations by the Lowell observers (Hardie and Giclas, 1955) indicate that for the 5-year period 1949–1954 the sun varied by less than ±0.4 per cent, the same upper limit obtained earlier by Stebbins and Jacobsen (1928). Such investigations should be continued to shed more light on the long-period variations suggested by the solar constant data.

The magnitude of the earth, as observed from the sun, may well show the largest variations of any of the planets, while variations with reduced

TABLE 9

PHOTOMETRIC DATA FOR PLANETS

	$V(1, 0)$	V_0	Variation Due to Rotation	Other Variations
Sun	−28.81	.....	.....	Constant within ±1.5 per cent
Mercury	− 0.36	.....	.....	.....
Venus	− 4.29	.....	Probably very small	.....
Earth	− 3.87	.....	Probable—irregular	Annual variation; short-period variations due to changing cloud coverage
Mars	− 1.52	− 2.01	Variable amplitude, about 0.15.	Probable annual variation; short-period variations due to changes in atmospheric transparency
Jupiter	− 9.25	− 2.55	Probable—irregular	Long-period variation correlated with change in surface features
Saturn	− 8.88	+ 0.67	Probably very small	No evidence of long-period variation
Uranus	− 7.19	+ 5.52	Suspected, but not confirmed	A small, long-period (84 years) variation expected due to oblateness and high obliquity of equator
Neptune	− 6.87	+ 7.84	Suspected, but not confirmed	No evidence of long-period variation
Pluto	− 1.01	+14.90	Amplitude 0.11	No evidence, but data limited

amplitude have been observed and are expected for Mars. In addition, Jupiter shows irregular variations over long periods, and Pluto a rotational variation of some 10 per cent. With these exceptions, after correction for distance and solar phase variation, the planets are remarkably constant in brightness; the variations suspected for the other planets have not been confirmed.

It is probable that accurate photoelectric observations of the planets, particularly in the blue region of the spectrum, will reveal small variations that are not apparent from the present data. It would appear that the amplitudes of such variations are less than the accuracy of visual or photographic photometric methods which can be profitably employed in other astronomical investigations.

5. MAGNITUDES AND COLORS OF THE SATELLITES

5.1. Introduction

The photometric data for the satellites in the solar system are still quite incomplete; in several cases only rough estimates of the mean opposition magnitudes, V_0, are available. Usually this scarcity of data is due to the satellite's proximity to a very much brighter planet or to its faintness, which makes observation difficult except with the largest telescopes.

For the satellites closest to their planets the scattered light makes it practically impossible to obtain accurate photoelectric or even photographic measures. For such objects, visual estimates of the magnitude difference between the inner and an outer satellite when nearly coincident will be the most reliable. In a few cases, where no new data were available, we have adopted the values given by Russell, Dugan, and Stewart (1945), denoted by the abbreviation RDS.

For the faintest satellites, only photographic magnitudes have been derived. These are listed in the text but have been converted to V magnitudes in the final compilation (Table 14, below) with the assumed mean color index of 0.8 mag. This conversion introduces an uncertainty in addition to that of the photographic magnitude scale.

5.2. The Moon

The detailed photometry of the moon is covered in chapter 6 of this volume. The most comprehensive study of the integrated brightness of the moon is that of Rougier (1933, 1937), who determined the variation with phase photoelectrically. The variation is not quite symmetrical, but the maximum difference between waxing and waning phases is only about

0.08 mag. near the quadratures. The mean variation can be expressed in the form

$$\Delta m\,(\alpha) = 3.05\left(\frac{\alpha}{100°}\right) - 1.02\left(\frac{\alpha}{100°}\right)^2 + 1.05\left(\frac{\alpha}{100°}\right)^3. \qquad (7)$$

There is considerable uncertainty in the magnitude of the full moon as defined by Rougier's phase-curve. Zöllner's (1865) accordant observations, made by comparing the moon with Capella and the moon with the sun, give $V_0 = -12.54$. Rougier's observations give $V_0 = -12.83$, and this is in reasonable agreement with that derived from Nikonova's (1949) photoelectric observations, which give $V_0 = -12.76$. The latter's observations also confirm the phase variation obtained by Rougier. Giving half-weight to Zöllner's visual observations, we obtain $V_0 = -12.74$, corresponding to $V(1, 0) = +0.21$.

Observations of a number of areas on the moon give a mean $B - V$ color of $+0.92$ with little difference between maria and bright regions. The mean $U - B$ color is $+0.46$ (Hardie, 1956).

5.3. The Satellites of Mars

The magnitudes and colors of the Martian satellites were observed by Kuiper at the 1956 opposition, when they were most favorably situated because of the close approach of the planet. The scattered light from Mars was still very large, and the results can be considered as only approximate ($\pm 0^m.1$). His observations give $V(1, 0) = 12.1$ for Phobos and $V(1, 0) = 13.3$ for Deimos, with $B - V = 0.6$ for both satellites. Reduced to mean opposition, these correspond to $V_0 = 11.6$ and 12.8, which are in good agreement with the earlier visual estimates.

5.4. The Satellites of Jupiter

Our knowledge of the variation in brightness of the Galilean satellites is quite complete, largely because of the extensive observational programs by Stebbins (1927) and by Stebbins and Jacobsen (1928). These observations were made with a quartz-potassium cell (maximum sensitivity for constant energy at 4600 A) and comparison stars of approximately the same color as the satellites. The magnitudes and colors of these stars have been observed at the McDonald Observatory, so that the Lick observations could be reduced to the V system. The 1926 series reduced with the linear relation, $V = Pe + 0.015 - 0.96(B - V)$, gives the mean opposition magnitudes shown in Table 10, while the 1927 series reduced with the relation, $V = Pe + 0.032 - 0.96(B - V)$, gives the mean opposition magnitudes shown in Table 11.

Magnitudes and colors of the satellites observed at the McDonald Observatory between 1950 and 1954 serve as a check on the reductions, and no difficulties were encountered for Jupiter II, III, and IV. It was not possible to effect a satisfactory transformation in the case of Jupiter I, for which the color is considerably redder than the comparison stars used and, moreover, varies with rotational phase.

Stebbins separated the variation in brightness with rotational phase from the solar phase variation by a method of successive approximations, and his results have been adopted in our discussion, except in the case of Jupiter IV, where we have redetermined the mean solar phase variation, using his individual observations.

5.41. *Jupiter I.*—The solar phase function (Stebbins and Jacobsen, 1928) is

$$\Delta m\,(a) = 0.046a - 0.0010a^2\,. \qquad (8)$$

From their observations in 1926 and 1927 the satellite was found to vary by about 0.21 mag., the leading side being the brighter. The McDonald observations made in 1951, 1952, and 1954 show considerable scatter but

TABLE 10

MEAN OPPOSITION MAGNITUDES OF JUPITER'S SATELLITES
(1926)

Object	P_e	V	$B-V$	V (Stebbins)
ι Cap	5.114	4.28	0.88	4.28
42 Cap	5.796	5.19	0.65	5.19
μ Cap	5.451	5.11	0.37	5.11
Jupiter I	5.802	.....	1.17 var.	4.69
J II	5.988	.....	0.87	5.17
J III	5.303	.....	0.83	4.53
J IV	6.263	.....	0.86	5.45

TABLE 11

MEAN OPPOSITION MAGNITUDES OF JUPITER'S SATELLITES
(1927)

Object	P_e	V	$B-V$	V (Stebbins)
20 Psc	6.334	5.44	0.96	5.44
27 Psc	5.720	4.84	0.94	4.85
44 Psc	6.544	5.72	0.90	5.71
Jupiter I	5.798	.....	1.17 var.	4.71
J II	5.976	.....	0.87	5.17
J III	5.293	.....	0.83	4.54
J IV	6.261	.....	0.86	5.47

indicate the same form of variation, with possibly somewhat smaller amplitude, as shown in Figure 6, *a*.

Slight color variations have been noted for other satellites, but the large variations in color with orbital phase for Jupiter I, shown in Figure 6, *b* and *c*, and amounting to 0.18 mag. in $B - V$ and 0.5 mag. in $U - B$, are outstanding.

The mean opposition magnitude from the McDonald observations is $\bar{V}_0 = 4.80$, which is 0.10 mag. fainter than given in Tables 10 and 11 but is to be preferred because of the uncertainty arising from the reduction of Stebbin's observations of this satellite to the V system.

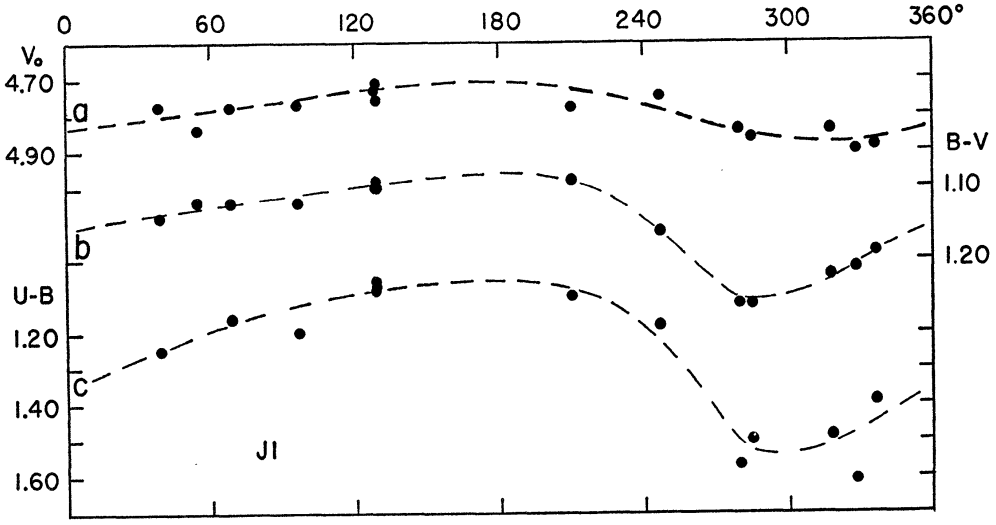

FIG. 6.—Variation of Io (Jupiter I) with rotational phase angle. (*a*) In yellow light, V_0; (*b*) in the $B - V$ color; (*c*) in the $U - B$ color. McDonald observations.

5.42 *Jupiter II.*—The solar phase function (Stebbins and Jacobsen, 1928) is

$$\Delta m\,(\alpha) = 0.0312\alpha - .00125\alpha^2\,. \qquad (9)$$

The variation with orbital phase obtained in 1927 is shown in Figure 7 as full-drawn lines, while the McDonald observations are plotted as circles and connected by dashes. The mean opposition magnitude is $\bar{V}_0 = 5.17$, and the $B - V$ color is 0.87 mag., showing no variation with orbital phase, θ. $U - B$ observations are available on 4 nights when θ was less than 180° and on 6 nights when θ was greater than 180°. Surprisingly, the mean $U - B$ color of the leading side is 0.43 mag., and of the trailing side 0.62 mag.; i.e., the trailing side is fainter in the ultraviolet by about 20 per cent.

5.43. *Jupiter III.*—The solar phase function (Stebbins and Jacobsen, 1928) is

$$\Delta m\,(\alpha) = 0.323\alpha - 0.00066\alpha^2\,. \qquad (10)$$

The variation with orbital phase obtained in 1927 is shown in Figure 8 as a line, while the McDonald observations are plotted as circles. The mean opposition magnitude is $\bar{V}_0 = 4.54$, the $B - V$ color is 0.83 mag. and shows no variation with orbital phase. The mean $U - B$ color is 0.51 mag., with evidence of only a slight variability. The average for the leading side is 0.48 mag. (4 nights) and the trailing side 0.52 mag. (10 nights).

5.44. *Jupiter IV.*—Stebbins and Jacobsen (1928) found the brightness variation of Jupiter IV to be exceptional, in that near opposition the satellite brightened up more on the leading side than on the trailing side. To demonstrate this phenomenon, we have plotted the three light-curves shown in Figure 9. Curve *a* is based on observations with $\alpha < 1^\circ.5$, *b* from observations with $2^\circ.7 < \alpha < 8^\circ$, and *c* from observations made with $\alpha > 8^\circ$. The phase function,

$$\Delta m\,(\alpha) = 0.078\alpha - 0.00274\alpha^2 \qquad (11)$$

makes the average of all the light-curves reduced to mean opposition $\bar{V}_0 = 5.50$, which is 0.04 mag. fainter than given in Tables 10 and 11.

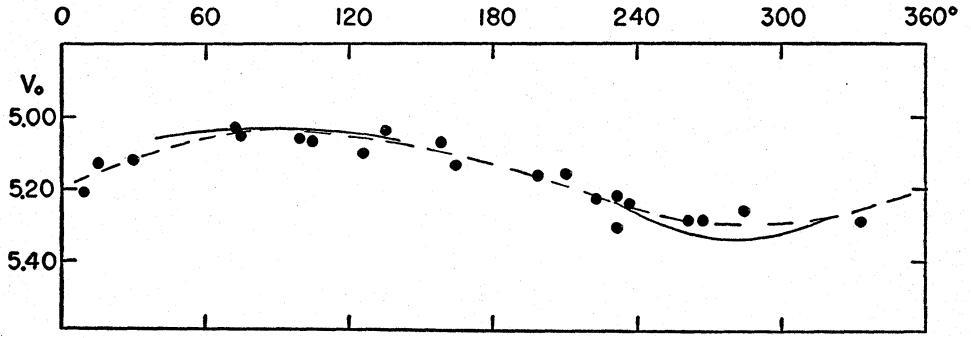

FIG. 7.—Variation of Europa (Jupiter II) in yellow light, V_0, with rotational phase angle. *Full-drawn curves:* Stebbins and Jacobsen (1927); *dashes and heavy dots:* McDonald observations.

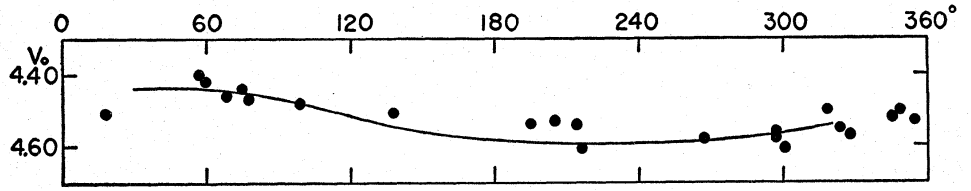

FIG. 8.—Variation of Ganymede (Jupiter III) in yellow light, V_0, with rotational phase angle. *Curve:* Stebbins and Jacobsen (1927); *dots:* McDonald observations.

Near opposition, the surface of Jupiter IV shows little variation with rotational phase, but, as the solar phase angle increases, the leading side decreases in brightness considerably more than does the trailing side. The McDonald color observations show no variation in either $B - V$ or $U - B$ with orbital phase or with difference in solar phase angle; the values of the colors are $B - V = +0.86$ and $U - B = +0.55$.

Comparing the decrease in brightness from opposition to $\alpha = 10°$, we find that for $\theta = 140°$ the decrease is 0.59 mag., while at $\theta = 250°$ it is only 0.41 mag. As Stebbins has noted, these changes in brightness are very large compared with those observed for other objects in the solar system. The moon shows a decrease of only 0.26–0.30 mag. over the same range.

As for the moon, the rapid decrease in brightness near opposition in Juipter IV is assumed to be due to small irregularities of the surface, casting shadows. It is therefore interesting that the leading side shows this effect more than the trailing side, possibly indicating a sweeping action through a particle cloud having a lesser angular velocity around Jupiter.

5.45. *The other satellites.*—The magnitude of Jupiter V is given as +13.0 in RDS. Van Biesbroeck and Kuiper (1946) have observed the satellite under moderately favorable conditions near western elongation and sug-

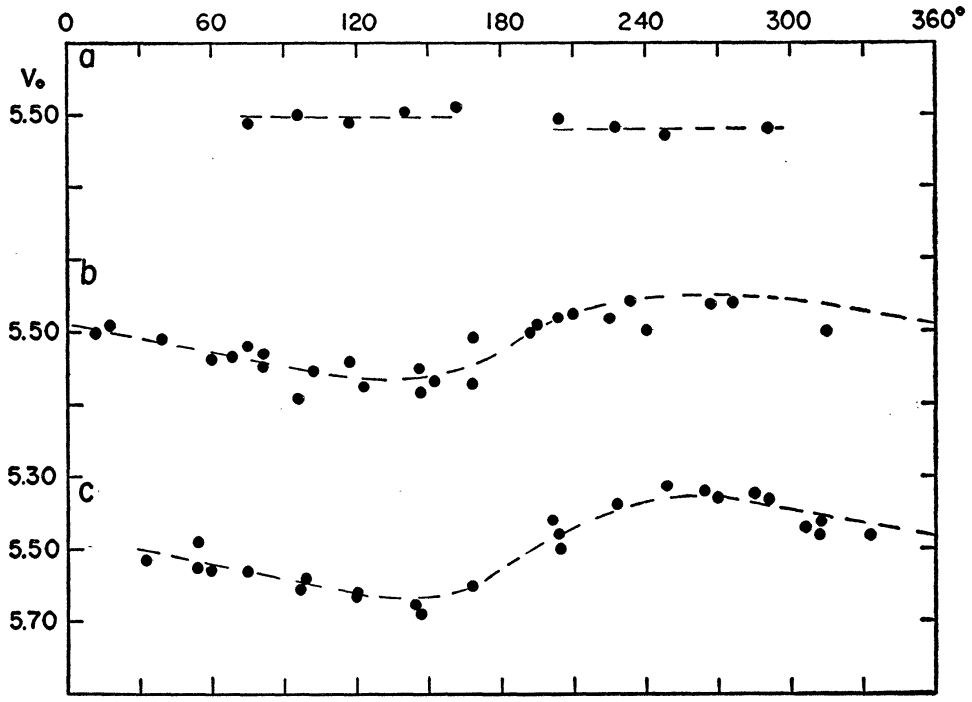

FIG. 9.—Variation of Callisto (Jupiter IV) in yellow light, V_0, with rotational phase angle. (*a*) Solar phase angle less than 1°.5; (*b*) solar phase angle between 2°.7 and 8°; (*c*) solar phase angle greater than 8°. Data by Stebbins and Jacobsen (1927).

gest that the satellite may be fainter than when it is near eastern elongation.

Jupiter VI is a moderately bright object, for which $V_0 = 13.7$ (RDS), and should be investigated for variation of brightness.

Jupiter VII is given as $V = 16$ in RDS, and no other determinations have been published.

The magnitudes of the last five satellites of Jupiter are given below and are photographic measures and estimates kindly made available by Dr. S. B. Nicholson for inclusion in this section. They are revisions of Nicholson's earlier values (published in the *Pub. A.S.P.*), based on corrections to the photographic magnitude scale indicated by recent photoelectric observations.

	P_g		P_g
Jupiter VIII.....	19.6	Jupiter XI.....	18.9
Jupiter IX.....	19.1	Jupiter XII.....	19.6
Jupiter X.....	19.4		

We have assumed a mean color index of 0.8 mag. for these objects to reduce them to V magnitudes.

5.5. The Satellites of Saturn

5.51. *Satellite I, Mimas.*—This satellite has not been measured photoelectrically because of its close proximity to the ring. The magnitude derived from earlier visual measures is about $\bar{V}_0 = 12.1$ (RDS).

5.52. *II, Enceladus.*—Two observations at McDonald (made in 1951, 1956) give $V_0 = 11.77$ and $B - V = 0.62$. No measures of the ultraviolet were obtained because of the proximity to the ring.

5.53. *III, Tethys.*—The magnitudes and colors based on four nights at McDonald (in 1951, 1953, 1956) are $V_0 = 10.27$, $B - V = 0.73$, $U - B = 0.34$.

5.54. *IV, Dione.*—The magnitudes and colors based on five nights at McDonald (in 1951, 1953, 1956) are $V_0 = 10.44$, $B - V = 0.71$, $U - B = 0.30$.

5.55. *V, Rhea.*—The mean magnitude and colors based on 11 nights at McDonald (in 1951, 1952, 1953, 1956) are $V_0 = 9.76$, $B - V = 0.76$, $U - B = 0.35$. Although the observations are not well enough distributed with regard to orbital phase (Fig. 10, *a*) to give a well-determined light-curve, it appears that the magnitude varies about 0.20; maximum (9.68) occurs near $\theta = 30°$ and minimum (9.88) near $\theta = 240°$. The colors show little or no variation.

5.56. *VI, Titan.*—The magnitudes and colors observed at McDonald on

19 nights from 1951 to 1956 give $V_0 = 8.39$, $B - V = 1.30$, $U - B = 0.75$. Although this satellite has been considered to be variable in light with a period equal to that of its revolution about Saturn and an amplitude of 0.24 mag. (Pickering, 1913), there is no definite evidence of a variation in our measures (Fig. 10, *b*). Examination of the observations by Wendell (1913) used by Pickering indicates that the assumed variation is probably due to the errors in the magnitudes of the comparison stars and not to a variation in the brightness of Titan. For example, Wendell measured

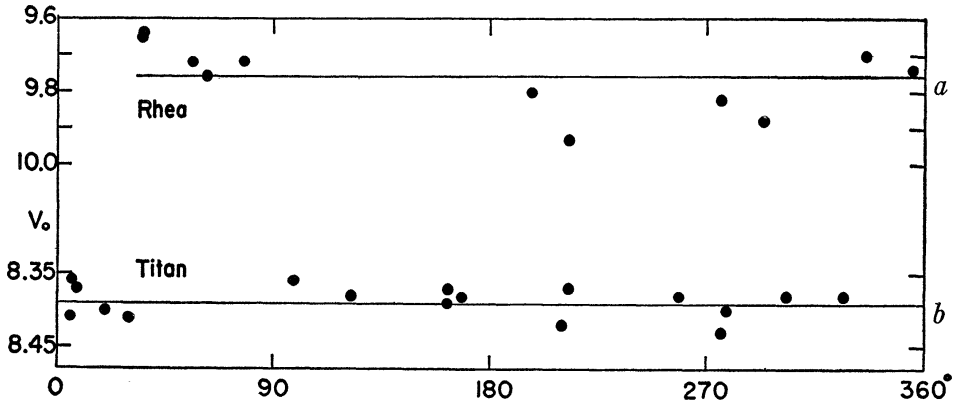

FIG. 10.—The yellow magnitudes, V_0, of Rhea and Titan as a function of rotational phase angle.

TABLE 12

WENDELL'S OBSERVATIONS, TITAN —(BD—21°4540)

Phase	Δm	Phase	Δm
23°.....	−0.535	201°.....	−0.535
67.....	− .535	246.....	− .535
90.....	− .49	269.....	− .555
113.....	− .51	337.....	−0.58
134.....	−0.52		

Titan with respect to BD −21°4540 on 9 nights when Saturn was near its stationary point. The magnitude differences listed in Table 12, on the assumption that Titan is constant in light, give a mean error of only ±0.024 mag. for one observation.

5.57. *VII, Hyperion.*—The mean magnitude of Hyperion as determined at McDonald in 1953 is $V_0 = 14.16$ (5*n*), while the colors are $B - V = 0.69$, $U - B = 0.42$:. The magnitude is considerably fainter than the earlier estimates.

5.58. *VIII, Iapetus.*—The variation in brightness of Iapetus is exceptional because of its large range of over 2 mag. It was discovered by J. D.

Cassini in 1671, who could see the satellite only at western elongation. Herschel could follow the satellite around the planet and obtained an approximate light-curve. A visual photometric light-curve was obtained by Pickering (1879). A more recent investigation by Widorn (1950) indicates that the brightness (not the magnitude) of the satellite can be represented quite well by the simple formula

$$H = 0.571 - 0.429 \sin\theta \qquad (12)$$

with the maximum occurring at western elongation.

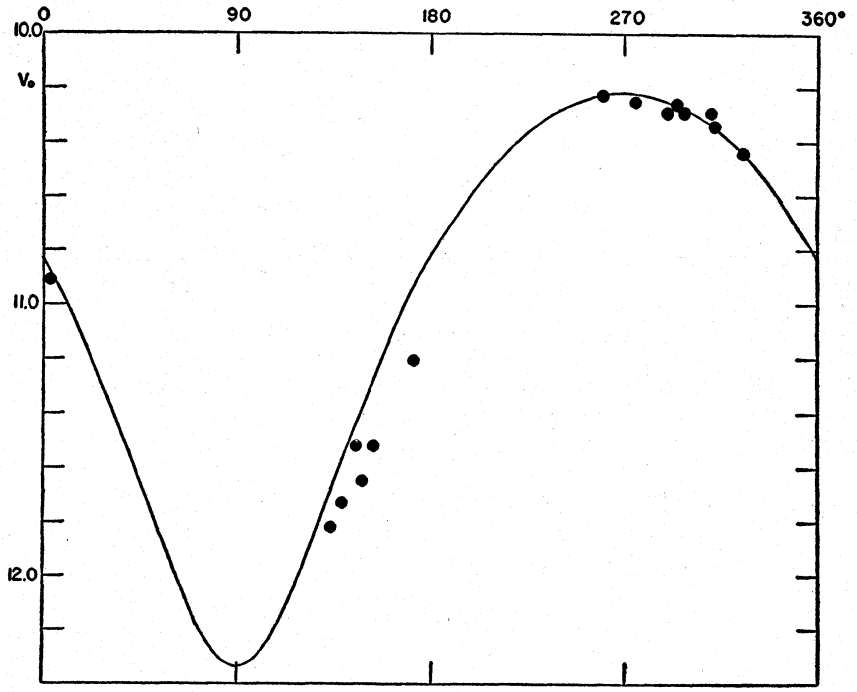

FIG. 11.—Variation of Iapetus in yellow light, V_0, with rotational phase angle. *Solid line:* Widorn's mean light-curve; *filled circles:* McDonald observations.

The satellite has been observed at McDonald on 17 nights from 1951 to 1953. These observations indicate a phase coefficient of about 0.03 mag/degree. The individual observations have been plotted in Figure 11, where Widorn's mean light-curve is shown as a solid line adjusted so that the maximum is 10.22 mag. In spite of the large range in magnitude, the colors are nearly the same at all phases; the mean colors for $0° < \theta < 180°$ are $B - V = 0.73$, $U - B = 0.30$, while for $180° < \theta < 360°$ the mean colors are $B - V = 0.69$, $U - B = 0.26$.

Widorn, from a consideration of his and earlier series of visual observa-

tions, has discussed the possibility that the light-curve of Iapetus is not constant in shape or mean magnitude. This must be further investigated, as the early observations appear to be rather unreliable.

5.6 The Satellites of Uranus

The magnitudes and colors of the two outer satellites of Uranus have been measured photoelectrically on 3 nights at McDonald. For the inner three satellites, Mr. T. Gehrels has determined the relative magnitudes from photographs taken with the 82-inch reflector. The results are given in Table 13.

5.7. The Satellites of Neptune

5.71. *Satellite I, Triton.*—The close satellite of Neptune is difficult to observe photometrically because of its proximity to the much brighter

TABLE 13

Magnitudes and Colors of Uranus Satellites

Satellite	V_0	$B-V$	$U-B$
V Miranda	16.5	.....	.....
I Ariel	14.4	.....	.....
II Umbriel	15.3	.....	.....
III Titania	14.01	0.62	0.25
IV Oberon	14.20	0.65	0.24

planet. Five observations made at McDonald (in 1950, 1951, 1953, 1956) give $V_0 = +13.55, B - V = 0.77, U - B = 0.40$. There is an indication that Triton's leading side is brighter than the following side by approximately 0.25 mag. Because of the limited number of observations and the difficulty in making them, this apparent variation is considered with reservation.

5.72. *II, Nereid.*—The distant satellite of Neptune has an apparent photographic magnitude of $Pg = 19.5$, determined by Kuiper. If its color is $B - V = 0.8$, the value of V_0 will be about 18.7.

5.8. Summary of Satellite Magnitudes

The magnitudes of the satellites reduced to unit distance, $V(1, 0)$, their mean opposition magnitudes, and remarks concerning their variability due to their rotation are summarized in Table 14. It appears that the periods of rotation that have been found are identical with the periods of

revolution of the satellites around their primaries, indicating that the satellites keep the same face toward the planet as does the moon.

Photometrically it is seen that the moon ranks seventh in brightness; the four Galilean satellites, Titan, and Triton are considerably brighter, while Rhea is equal to the moon.

The two satellites of Mars and the outer satellites of Jupiter are intrinsically the faintest objects, and it is obvious that their discovery is due to the comparative proximity to the earth; Deimos at a distance of Neptune would be an object of the twenty-eighth magnitude.

TABLE 14

SUMMARY OF SATELLITE MAGNITUDES

	Satellite	$V(1, 0)$	$\bar{V}_0$	Rotational Variation (Mag.)
	Moon	+ 0.21	−12.74	±0.08*
Mars	I Phobos	+12.1	+11.6	.....
	II Deimos	+13.3	+12.8	.....
Jupiter	V	+ 6.3	+13.0	.....
	I Io	− 1.90	+ 4.80	0.21
	II Europa	− 1.53	+ 5.17	0.34
	III Ganymede	− 2.16	+ 4.54	0.16
	IV Callisto	− 1.20	+ 5.50	0.16†
	VI	+ 7.0	+13.7	.....
	VII	+ 9.3:	+16	.....
	VIII	+12.1‡	+18.8‡	.....
	IX	+11.6‡	+18.3‡	.....
	X	+11.9‡	+18.6‡	.....
	XI	+11.4‡	+18.1‡	.....
	XII	+12.1‡	+18.8‡	.....
Saturn	I Mimas	+ 2.6	+12.1	.....
	II Enceladus	+ 2.22	+11.77	.....
	III Tethys	+ 0.72	+10.27	.....
	IV Dione	+ 0.89	+10.44	.....
	V Rhea	+ 0.21	+ 9.76	0.20
	VI Titan	− 1.16	+ 8.39	.....
	VII Hyperion	+ 4.61	+14.16	.....
	VIII Iapetus	+ 1.48	+11.03	2.12
Uranus	V Miranda	+ 3.8	+16.5	.....
	I Ariel	+ 1.7	+14.4	.....
	II Umbriel	+ 2.6	+15.3	.....
	III Titania	+ 1.30	+14.01	.....
	IV Oberon	+ 1.49	+14.20	.....
Neptune	I Triton	− 1.16	+13.55	0.25:
	II Nereid	+ 4.0‡	+18.7‡	.....

* Slight difference between waxing and waning phases.

† For $\alpha > 8°$; small near opposition.

‡ Pg magnitudes reduced with a mean color index +0m8.

6. COLOR MEASUREMENTS

6.1. The Sun

Because of the difficulties encountered in determining the color of the sun directly, we generally assume that its colors are the same as those of stars with the same spectral type and luminosity. The spectral type of the sun has been determined by Keenan and Morgan (1952) to be G2 V; it refers to the solar spectrum as reflected from one of Jupiter's satellites and is directly comparable with spectra of stars.

As the relationship between spectral type and color is well defined for MK types (e.g., Morgan, Harris, and Johnson, 1953), the mean values of G2 V, $B - V = +0.63$ and $U - B = +0.14$, should closely approximate the colors of the sun. The values of $V - R = 0.45$ and $R - I = 0.29$ were derived by Hardie (1956).

Stebbins and Kron (1956) have determined the $B - V$ color index of the sun directly in conjunction with their determination of the magnitude of the sun (Sec. 2). Their adopted value of 0.636 ± 0.006 (m.e.) for $B - V$ agrees with the value based on the spectral type.

6.2 The Planets

The colors used in this chapter are based on two unpublished sources: the McDonald measures of U, B, V and the R and I values derived by

TABLE 15

MEAN COLORS OF THE PLANETS

Planet	$U-B$	$B-V$	$V-R$	$R-I$
Sun	0.14	0.63	+0.45	+0.29
Mercury	.....	0.93	+0.85	+ .52
Venus	.50	0.82	.....	.....
Mars	.58	1.36	+1.12	+ .38
Jupiter	.48	0.83	+0.50	− .03
Saturn	.58	1.04	.....	.....
Uranus	.28	0.56	−0.15	− .80
Neptune	.21	0.41	−0.33	− .80
Pluto	0.27	0.80	+0.63	+0.28

Hardie at the McDonald and Lowell Observatories, kindly made available in advance of publication. They are collected in Table 15.

Table 16 gives the corresponding difference, planet − sun, for each wave-length region, the values of ΔV being taken equal to zero. The data of Table 16 are plotted in Figure 12, which therefore represents the reflectivity as a function of wave length on a logarithmic scale.

The observed colors for Mercury are rather uncertain, as the observa-

TABLE 16

COLOR DIFFERENCES BETWEEN PLANETS AND SUN

Planet	*U*	*B*	*V*	*R*	*I*
Neptune.....	−0.15	−0.15	0.00	+0.78	+1.87
Uranus.....	+0.07	− .07	.00	+ .60	+1.69
Pluto.....	+0.30	+ .17	.00	− .18	−0.17
Venus.....	+0.55	+ .19	.00	.....	.....
Jupiter.....	+0.54	+ .20	.00	− .05	+0.27
Mercury.....	.....	+ .30	.00	− .40	−0.63
Saturn.....	+0.85	+ .41	.00	.....	.....
Mars.....	+1.17	+0.71	0.00	−0.67	−0.76

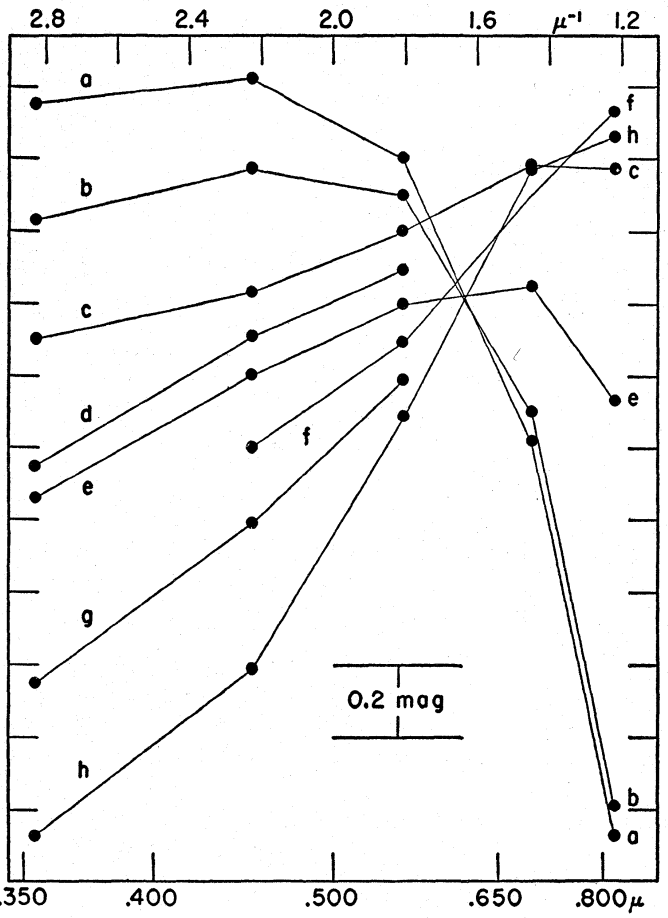

FIG. 12.—Wave-length dependence of the reflectivity of the planets. (*a*) Neptune; (*b*) Uranus; (*c*) Pluto; (*d*) Venus; (*e*) Jupiter; (*f*) Mercury; (*g*) Saturn; (*h*) Mars.

tions have to be made against a bright sky or at twilight when the zenith distance is large. The values for Mars are based on the results at two oppositions and have been freed from the effects due to rotation. For Saturn the color of the combined ball and ring depends on the appearance of the ring, as the latter is considerably bluer than the planet alone. The values given in the table are extrapolations obtained from measures when the inclination of the ring to the line of sight was small to "no-ring."

It must be remembered that our colors are based on broad-band filters and are affected by differences in absorption bands. The first two planets plotted in Figure 12 show that the effect of the absorption bands is very prominent in the R and I measures and is also present to a lesser extent in the V measures.

In the case of Mars we have additional data concerning the variation of color with wave length from the monochromatic magnitudes by Woolley and collaborators (1953, 1955), made during the 1952 and 1954 oppositions. The results obtained in 1954 are plotted in Figure 13, *a*, as circles

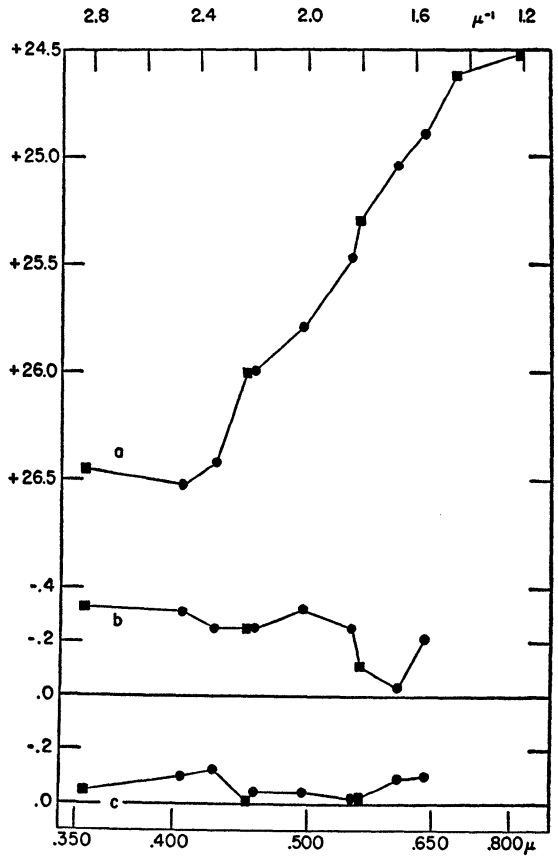

FIG. 13.—(*a*) Wave-length dependence of the mean reflectivity of Mars. (*b*) Deviations for abnormal night, May 3–4, 1952, from mean curve. (*c*) Deviations for nearly normal nights, March 8 and 12, 1952, from mean curve. Squares are Woolley's (1954) observations of monochromatic magnitude differences, Mars — sun; circles are photoelectric means.

and show good agreement with the photoelectric values plotted as squares. It is of interest to note that the observed U point is brighter than the observation at 0.405 μ, indicating the presence of Rayleigh scattering in the Martian atmosphere.

The Mount Stromlo opposition magnitudes and phase coefficients derived for 1952 appear adversely affected by the observations of May 3–4, 1952, when the planet was close to opposition ($\alpha = 2^\circ.5$). Fortunately, McDonald observations were secured on that same night, and the two sets are accordant. They show that the brightness and the color of Mars on that night were abnormal. We have plotted the differences, May 3–4, 1952, *minus* normal, in Figure 13, *b*, from which it is seen that both the Mount Stromlo and the McDonald data differ systematically from the remainder of the observations. On May 3–4, 1952, the planet was both brighter and bluer than normal. A similar comparison was made for more typical nights, March 8 and 12, 1952, as shown in Figure 13, *c*. The abnormal nature of the night May 3–4 is apparent. These conditions may have been extreme, but variations of a smaller amount may be more common; such variations have been noted by Johnson and Gardiner (1955).

6.3 The Satellites

The adopted values of the colors of the satellites are given in Table 17, while the differences, satellites − sun, are given in Table 18. These latter results are plotted in Figure 14, in a manner similar to that for the planets.

The results for Oberon and Titania, though not of high weight because of the proximity to Uranus and their apparent faintness, show that the surfaces of these satellites must be nearly neutral reflectors of solar radiation. In general, the surface reflectivity is higher in the red part of the spectrum than in the blue and ultraviolet, the extreme example being that of Io.

The bottom two curves—those of the moon and Titan—are of particular interest in that they represent spectral distributions for a satellite without an atmosphere and one with an atmosphere. The effect of the atmosphere is apparent in the ultraviolet but is very obvious in the infrared, where the methane absorption bands are prominent.

For the faintest satellites, only photographic magnitudes are available at present; they have been reduced to visual with the median value of +0.75 for $B - V$ obtained from the brighter satellites without atmospheres. Because of the exceptional behavior of Io, some uncertainty is attached to this reduction.

TABLE 17

COLORS OF THE SATELLITES

Satellite	$U-B$	$B-V$	$V-R$	$R-I$	Remarks
Earth:					
Moon	0.46	0.92	0.80	0.46	Variable over surface
Mars:					
I Phobos	.....	0.6	.....	.....	
II Deimos	.....	0.6	.....	.....	
Jupiter:					
I Io	1.30	1.17	.66	.32	Variable colors
II Europa	0.52	0.87	.57	.31	$U-B$ variable
III Ganymede	0.50	0.83	.59	.31	Nearly constant
IV Callisto	0.55	0.86	.61	.32	Constant
Saturn:					
II Enceladus	.....	0.62	.....	.....	
III Tethys	0.34	0.73	.....	.....	
IV Dione	0.30	0.71	.48	.32	
V Rhea	0.35	0.76	.61	.26	Constant
VI Titan	0.75	1.30	.88	.11	Constant
VIII Iapetus	0.28	0.71	.....	.....	Nearly constant
Uranus:					
III Titania	0.25	0.62	.52	.41	
IV Oberon	0.24	0.65	.49	.33	
Neptune:					
I Triton	0.40	0.77	0.58	0.44	

TABLE 18

DIFFERENCE IN COLORS: SATELLITE — SUN

Satellite	U	B	V	R	I	n
Earth:						
Moon	0.61	+0.29	0.00	−0.35	−0.52	9
Jupiter:						
I Io	1.70	+ .54	.00	− .21	− .24	10
II Europa	0.62	+ .24	.00	− .12	− .14	8
III Ganymede	0.56	+ .20	.00	− .14	− .16	6
IV Callisto	0.64	+ .23	.00	− .16	− .19	7
Saturn:						
IV Dione	0.24	+ .08	.00	− .03	− .06	3
V Rhea	0.34	+ .13	.00	− .16	− .13	4
VI Titan	1.28	+ .67	.00	− .43	− .25	11
Uranus:						
III Titania	0.10	− .01	.00	− .07	− .19	1
IV Oberon	0.12	+ .02	.00	− .04	− .08	2
Neptune:						
I Triton	0.40	+0.14	0.00	−0.13	−0.28	5

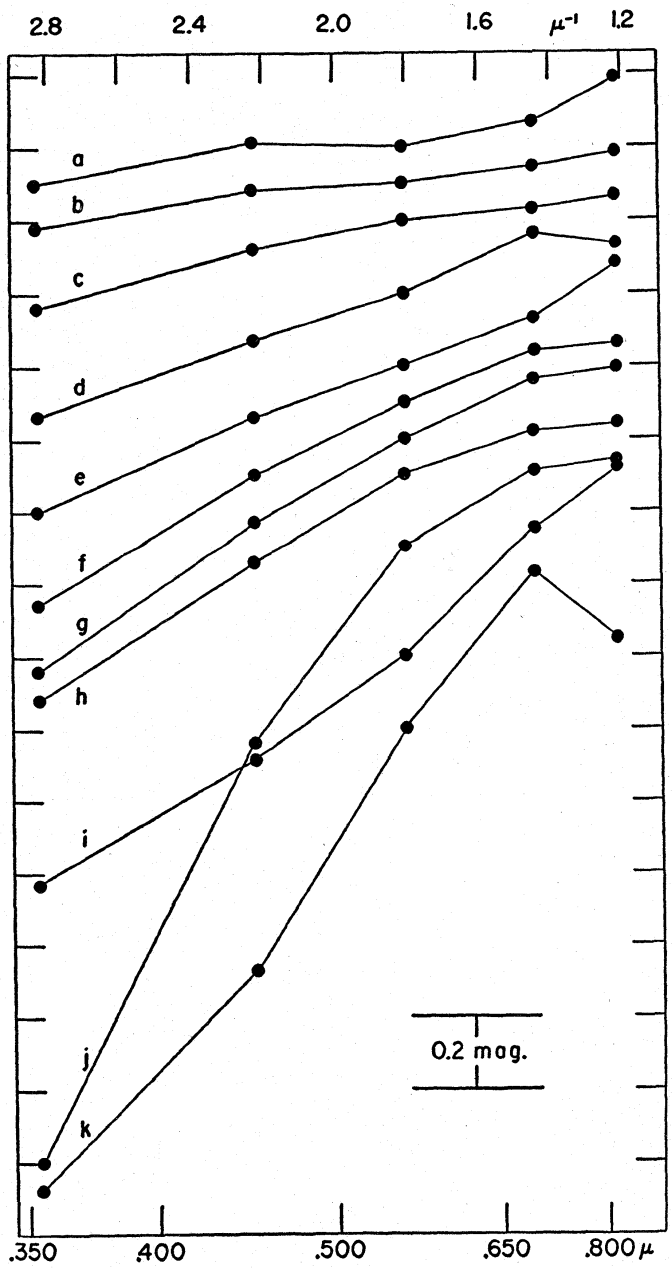

FIG. 14.—Wave-length dependence of the reflectivity of the satellites. (*a*) Titania; (*b*) Oberon; (*e*) Dione; (*d*) Rhea; (*c*) Triton; (*f*) Ganymede; (*g*) Callisto; (*h*) Europa; (*i*) moon; (*j*) Io; (*k*) Titan.

6.4. Observations of the Planets and Satellites in the Infrared

The observed energy distribution of the planets between 1.0 and 2.5 μ has been studied by Kuiper (1952, pp. 351 ff.) with a lead sulfide photoconductive cell and a spectrometer. From the published curve (Kuiper, 1952, Fig. 85) for the moon, the effects of the strong terrestrial water-vapor bands illustrate the difficulty of interpretation of broad-band photometry in this region, especially as these bands are variable in strength.

From the published curves for Mercury the effect of planetary radiation temperature is apparent in the region near 2.1 μ. For Mars the comparison with the moon shows that, with the relative intensities adjusted so that they are equal at 1.3 μ, Mars is about 1.5 times as bright as the moon at 0.8 μ and only 0.5 times as bright at 2.1 μ; i.e., Mars is much "bluer" than the moon in the infrared, contrary to the difference in the blue visual region.

For Venus, and particularly Jupiter and Saturn, respectively, there are additional infrared absorptions by CO_2 and by CH_4 and NH_3. The relative energy distributions of Jupiter and Saturn, however, are quite different in the infrared, Jupiter being much the "bluer" of the two.

Kuiper (1956*b*) has measured the intensities of several of the planets and satellites at 1 and 2 μ, using a lead sulfide cell and broad-band filters. This method does not give the detailed information that is obtained from the spectrometer observations, but the limiting magnitude is much fainter.

The results for the planets and satellites are given in Table 19, where the data are presented in the form $I(2\,\mu)/I(1\,\mu)$. This ratio has been adjusted so that the mean for a number of stars with average spectral type close to that of the sun is 1.

TABLE 19

Infrared Observations of Planets and Satellites

Planet or Satellite	$I(2\mu)/I(1\mu)$	Planet or Satellite	$I(2\mu)/I(1\mu)$
Sun	1.00	Mars	1.00
Venus	1.61	Io	1.06
Saturn	0.47	Europa	0.66:
Saturn's Ring	0.45	Ganymede	0.63
Jupiter	0.21	Callisto	0.95
Uranus	0.06:	Titan	0.20:
Mercury	3.5		

The large value of the ratio, $I(2\,\mu)/I(1\,\mu)$, observed for Mercury is due to planetary radiation (see above). Venus is also relatively bright at 2 μ, but the absorption bands in Saturn, Jupiter, and especially Uranus reduce

the intensity at 2 μ considerably below that of the incident radiation from the sun.

For the satellites the methane atmosphere of Titan (Kuiper, 1944, 1952) reduces the intensity at 2 μ below that of Jupiter's satellites. Whether the lower values of Jupiter II and III are to be attributed to similar absorption must await further observations. At the present time no atmospheres have been definitely found for them, but Kuiper (1952, p. 309) does not regard the matter as closed.

7. ALBEDOS OF THE PLANETS AND SATELLITES

7.1 Introduction

Of the several possible definitions of *albedo* (Schönberg, 1929), the ratio of the total flux reflected in all directions to the total incident flux, suggested by Bond (1861) and adopted by Russell (1916*b*), appears to be most suitable for use in the discussion of the planets and satellites.

Consider the planet to be at unit distance from the sun and the earth. Then the apparent diameter at unit distance, σ_1 radians, and the incident solar flux per unit area, πF, give the total flux incident on the planet,

$$\pi F \sigma_1^2 .$$

Let $j(\alpha)\sigma_1^2$ be the flux reflected by the planet in the direction of the earth in which α is the phase angle; then the total flux reflected in all directions is

$$2\pi \int_0^\pi j(\alpha)\, \sigma_1^2 \sin \alpha d\alpha .$$

The *Bond albedo*, A, is given by

$$A = \frac{2}{\pi F}\int_0^\pi j(\alpha) \sin \alpha d\alpha = \frac{j(0)}{\pi F} \times 2\int_0^\pi \Phi(\alpha) \sin \alpha d\alpha = pq . \quad (13)$$

The factor p, which is called the *geometric albedo*, can be easily evaluated, since

$$m(1, 0) = \text{Constant} - 2.5 \log j(0)\, \sigma_1^2 \quad (14)$$

and

$$m(\text{sun}) = \text{Constant} - 2.5 \log \pi F , \quad (15)$$

so that

$$\log p = 0.4\,[m(\text{sun}) - m(1, 0)] - 2 \log \sigma_1 . \quad (16)$$

If the mean radius of a planet is expressed in terms of the earth's mean radius, R/R_E,

$$\sigma_1 = \frac{R}{R_E} \sin 8''.79 \quad (17)$$

and

$$\log p = 0.4\,[m(\text{sun}) - m(1, 0)] - 2 \log \frac{R}{R_E} + 8.741 . \quad (18)$$

The factor q, which is called the *phase integral*, can be computed from the observed variation in brightness with solar phase angle for Mercury, Venus, earth, and the moon but must be estimated from theoretical considerations for the remaining objects.

7.2 The Geometric Albedos of the Planets

Provisional values of the mean radii of the planets as given by Kuiper are listed in the second column of Table 20. Using the values of $V(1, 0)$ given in Table 9 with the adopted value of V (sun) $= -26.81$, the computed values of $p(V)$ listed in Table 20 follow from the definition of p. These values have been computed to three figures although an uncertainty of ± 0.05 mag. in V (sun) introduces an uncertainty of nearly 5 per

TABLE 20

Albedos of the Planets

	R/R_E	$p(U)$	$p(B)$	$p(V)$	$p(R)$	$p(I)$	q_V	$A_{(V)}$
Mercury..	0.38	.....	0.076	0.100	0.145	0.179	0.563	0.056
Venus....	0.961	0.353	.492	.586	.....	.....	1.296	.76
Earth....	1.000	.....	.....	.367	.....	.....	1.095	.36*
Mars.....	0.523	.052	.080	.154	.286	.310	1.04	.16
Jupiter...	(11.20, 10.46)	.270	.370	.445	.466	.347	1.65	.73
Saturn...	(9.48, 8.48)	.211	.316	.461	.....	.....	1.65	.76
Uranus...	3.72	.530	.603	.565	.325	.119	1.65	.93
Neptune..	3.38	.585	.624	.509	.248	.091	1.65	.84
Pluto.....	0.45	0.099	0.111	0.130	0.154	0.152	1.04	0.14

* See text.

cent in p, while additional uncertainty is introduced in the case of Mercury and Pluto, whose diameters are not well determined.

For the other wave-length regions the differences in color, planet − sun (Table 16), give the values of $p(U), \ldots, p(I)$ listed in the table. For Mars, the monochromatic measures by Woolley and his collaborators (1955) provide additional information regarding the variation of p with wave length for this planet. The results derived from their data, using Kuiper's diameter for Mars and our adopted value of V(sun), are listed in Table 21.

The values of p have been plotted against reciprocal wave length in Figure 15. The lines connecting the observed points for the planets Mercury, Mars, and Pluto are probably rather reliable indications of the variation of p with wave length. However, for the remaining planets the presence of strong atmospheric absorption bands makes the variation of p with wave length irregular.

7.3 The Bond Albedos of the Planets

The visual Bond albedo for each planet is listed in the last column of Table 20, based on the values of the phase integral, q, given in the penultimate column. For the first three planets the values of q have been derived from the observed phase-curves. For Mars (and the asteroids) we have followed a suggestion by Russell (1916*b*), who noted that the ratio of $q/\Phi(50°)$ was nearly constant. From the modern phase-curves for Mercury, Venus, earth, and moon we find that $q = 2.17\Phi(50°)$ represents the observed values very well; and the value derived for Mars (and the asteroids) from the slight extrapolation of the observed phase-curve should be reliable. The value of q adopted for Pluto is that derived for Mars, although it is possible that a value nearer to that found for Mercury would be more appropriate.

TABLE 21

MONOCHROMATIC ALBEDOS OF MARS
(After Woolley)

	λ(A)						
	4050	4250	4550	4945	5430	5980	6360
$p(\lambda)$.....	0.049	0.054	0.081	0.097	0.131	0.194	0.227
$q(\lambda)$.....	.95	.99	1.04	1.09	1.19	1.25	1.31
$A(\lambda)$.....	0.047	0.053	0.084	0.106	0.16	0.24	0.30

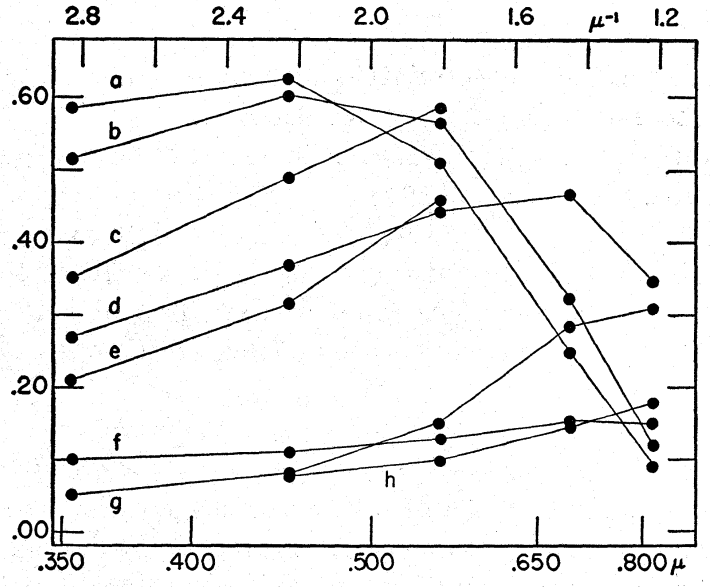

FIG. 15.—Wave-length dependence of the geometrical albedos of planets. (*a*) Neptune; (*b*) Uranus; (*c*) Venus; (*d*) Jupiter; (*e*) Saturn; (*f*) Pluto; (*g*) Mars; (*h*) Mercury.

From the major planets, Russell (1916*b*) assumed $q = 1.50$, which obtains for Lambert's law of diffuse reflection. Based on the discussion of theoretical phase-curves in Section 8, we have adopted $q = 1.65$ for the phase integral in the visual region.

The Bond albedos have not been tabulated for wave-length regions other than the visual because of the uncertainty in the phase integral that should be used. Only in the case of Mars are there data concerning the variation of q with wave length, based on Woolley's (1955) observations and tabulated in Table 21. For the major planets the theoretical discussion in Section 8 indicates that q probably decreases slightly with increasing wave length, while for Venus the low value found for the visual region is probably applicable also in the blue and ultraviolet. It would be desirable to observe the phase-curves for Mercury, Venus, earth, moon, and Mars in wave-length regions other than the visual region and to obtain accurate limb-darkening-curves for Jupiter and Saturn in different colors, so that the Bond albedos could be made more reliable.

For the earth, the visual albedo determined from p and q is 0.40, but the value given in Table 20 is 0.36, based on the discussion by Danjon in Volume **2**, chapter 15, Section 3; the former value is based on observations made in France only, while the latter is a mean value for the entire earth.

It has been pointed out by several investigators (e.g., Sharonov, 1939) that the evaluation of the Bond albedo in the manner outlined in Section 7.1 is only approximate, in that it assumes that the brightness of the planet depends only on the phase angle, α, e.g., that the surface has uniform properties of diffuse reflection. This is obviously not true, for example, in the case of Mars with regard to its north or south poles; but it is difficult to see how such effects of non-uniformity could be quantitatively allowed for.

7.4 Albedos of the Satellites

The values of the geometric albedos, p, for the satellites tabulated in Table 22 are derived from the mean radii given by Kuiper (see Vol. **5** of this series), the values of $V(1, 0)$ given in Table 14, and the color differences given in Table 18. These values are also plotted in Figure 16.

The value of the phase integral required in the determination of the Bond albedo is known only for the moon, for which $q = 0.585$; this has been adopted in the table for all the satellites.

The high values of the geometric albedo for the Saturn satellites are well known, but the extremely high values for Jupiter I and II have not been pointed out before. The magnitudes of Jupiter II, III, and IV as derived from Stebbins' observations in 1926 and 1927 and the magnitudes

TABLE 22

ALBEDOS OF THE SATELLITES

	R/R_E	$p(U)$	$p(B)$	$p(V)$	$p(R)$	$p(I)$	q	A_V
Moon.....	0.273	0.066	0.088	0.115	0.16	0.17	0.585	0.067
Jupiter I....	.255	.19	.56	.92	1.12	1.15	.585	.54
Jupiter II...	.226	.47	.67	.83	0.93	0.95	.585	.49
Jupiter III..	.394	.29	.41	.49	0.56	0.57	.585	.29
Jupiter IV..	.350	.14	.21	.26	0.30	0.31	.585	.15
Mimas.....	.04:	.....	.....	.49	.....	.....	.585	.29
Enceladus..	.05:	.....	.53	.54	.....	.....	.585	.32
Tethys.....	.08	.64	.76	.84	.....	.....	.585	.49
Dione.....	.07:	.75	.87	.94	0.96	0.99	.585	.55
Rhea.....	.120	.60	.73	.82	0.96	0.93	.585	.48
Titan.....	.377	.06	.12	.21	0.32	0.27	.585	.12
Triton.....	0.29	0.25	0.32	0.36	0.41	0.47	0.585	0.21

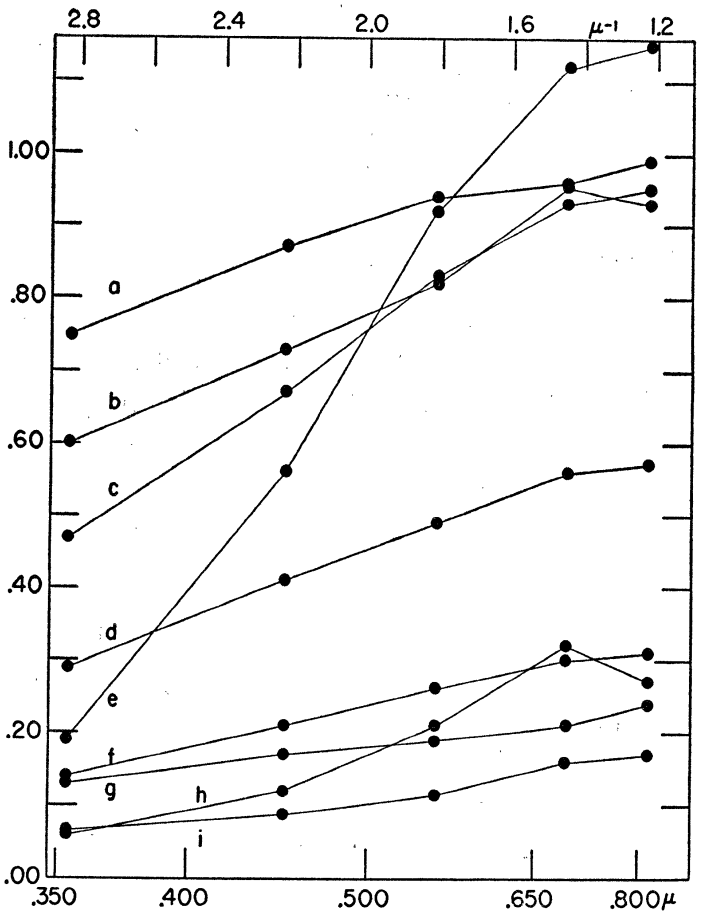

FIG. 16.—Wave-length dependence of the geometrical albedos of satellites. (*a*) Dione; (*b*) Rhea; (*c*) Europa; (*d*) Ganymede; (*e*) Io; (*f*) Callisto; (*g*) Triton; (*h*) Titan; (*i*) moon.

Note added in proof: To be consistent with the value now accepted for the radius of Triton, the albedos shown above (*g*) should be multiplied by 1.9 (see Table 22).

observed at the McDonald Observatory agree in making these satellites considerably brighter than the earlier measures by visual observers. In the case of Jupiter I the reduction of Stebbins' observations to the V system was uncertain and would make this satellite even brighter than the adopted value in Table 22, which is based on the McDonald measures.

8. THEORETICAL LIMB DARKENING, PHASE VARIATIONS, AND ALBEDOS

8.1 Introduction

The observations of planets' and satellites' brightness at various phase angles, α, enable one to determine the Bond albedo, A, as summarized in Section 7. It was shown that the albedo could be expressed as a product of two factors, p and q, where the factor p depends only on observations made at full phase and can be derived for all the planets and satellites whose diameters are known. The factor q, on the other hand, can be derived from observations only in the cases of Mercury, Venus, earth, and the moon; for the major planets the factor must be estimated from theoretical considerations, guided in part by observations of limb darkening.

In surveying the theoretical aspects of planetary photometry, we consider three types of "model planets": (*a*) planets with optically thick atmospheres (Secs. 8.4–8.6); (*b*) planets with no atmosphere (Sec. 8.7); and (*c*) planets with optically thin atmospheres (Sec. 8.8). The "models" are assumed to be spherical and to possess homogeneous atmospheres and surfaces. As the real planets are not strictly spherical, their atmospheres not homogeneous, and their surfaces not without definite features, we must consider the results as applying to the average or smoothed-out characteristics of the real objects. This is obviously true for the reflective properties of the lunar surface and the limb darkening of Jupiter with its belts; but it is true also in the case of a rotating planet where convection currents from the bright to the dark side may cause differences of particle size, which affect the brightness systematically over the surface (e.g., van de Hulst, 1952, p. 91).

8.2 Definitions

The co-ordinates of a point on the surface of a planet can be described in terms of a longitude, ω, and a latitude, ψ (Fig. 17). In photometric investigations the natural great circle to employ is that one which passes through the subsolar point, S, and the subterrestrial point, E; longitude is measured along this intensity equator from the subterrestrial point, while latitude is measured along meridians perpendicular to this equator. The

longitude of the subsolar point is the solar phase angle, α, already referred to in our discussions of the phase variations of the planets.

For any point on the surface, $P(\omega, \psi)$, we have

$$\mu = \cos \epsilon = \cos \psi \cos \omega ,$$
$$\mu_0 = \cos i = \cos \psi \cos (\omega - \alpha) , \tag{19}$$

where i and ϵ are the angles of the incidence and reflection. Let the angle EPS equal $\pi - \phi$, where ϕ is the azimuthal angle of the reflected ray, given by

$$\cos \phi = \frac{\cos \epsilon \cos i - \cos \alpha}{\sin \epsilon \sin i} , \qquad \sin \phi = \frac{\sin \psi \sin \alpha}{\sin \epsilon \sin i} . \tag{20}$$

At full phase, $\alpha = 0°$, and all points have $\mu = \mu_0$ and $\phi = 180°$.

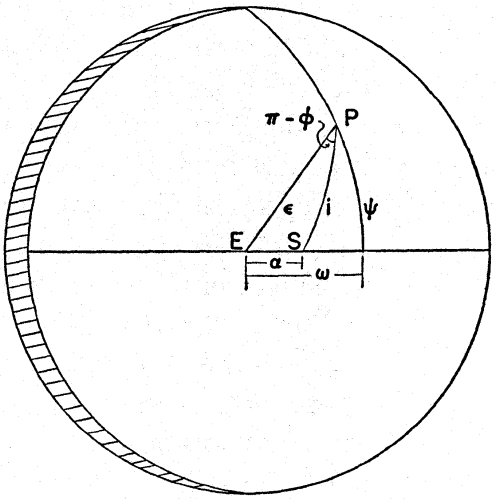

FIG. 17.—Co-ordinate system for photometric investigations of planets

Because of the great distances of the planets from the earth, the apparent disk of the planet is an orthographic projection on the plane of the sky. If R is the apparent radius of the planetary disk, the distance of a point from the center, E, of the disk may be expressed in terms of $r/R = \sin \epsilon$.

8.3 The Principle of Reciprocity

The principle of reciprocity, first formulated by Helmholtz, has been discussed with regard to planetary photometry by Minnaert (1941, 1946). If we consider a point, $P(\omega, \psi)$, on the planet when the solar phase angle is α, we may express the intensity at this point either as $I(\mu, \phi; \mu_0)$ or as $I(\mu, \mu_0, \alpha)$. The first form is generally used in theoretical discussions, but Minnaert has commented on the fact that the latter notation is convenient

in photographic photometry of planets, since, for a given photograph, a is constant.

According to the principle of reciprocity, a planet having a surface with homogeneous photometric properties will satisfy the relation

$$\frac{I(\mu, \mu_0, a)}{\mu_0} = \frac{I(\mu_0, \mu, a)}{\mu}, \tag{21}$$

where we have merely interchanged the angles of incidence and reflection.

It is seen that this principle of reciprocity permits one to check the homogeneity of a planetary atmosphere and/or surface, irrespective of the specific form of the law of reflection. If the reciprocity principle is not satisfied, one must look for an explanation outside the scope of the present remarks (see also chap. 6).

8.4 Planets with Optically Thick Atmospheres

As van de Hulst (1952) remarks, a deductive theory of scattering in a planetary atmosphere consists of three distinct parts:

(i) The properties of single scattering have to be computed from the assumed composition and particle size. For those small compared with the wave length of light, the Rayleigh scattering formulae are applicable, while for larger particles Mie's formulae must be used. As the exact formulae are complex and depend on the unknown particle size, it is convenient to assume simple analytical forms for the particle phase function, $f(\cos\Theta)$, where $\Theta = \pi - a$ is the angle between the incident ray and the reflected ray. We shall have occasion to refer to the following phase functions:

Rayleigh scattering with allowance for polarization:	$f_l(\cos\Theta) = \frac{3}{4}\cos^2\Theta$, $f_r(\cos\Theta) = \frac{3}{4}$;
Rayleigh phase function:	$f(\cos\Theta) = \frac{3}{4}\varpi_0(1+\cos^2\Theta)$;
Isotropic scattering:	$f(\cos\Theta) = \varpi_0$;
Anisotropic scattering:	$f(\cos\Theta) = \varpi_0(1 + a\cos\Theta)$.

The last three are special cases of

$$f(\cos\Theta) = \varpi_0 + \varpi_1 P_1(\cos\Theta) + \varpi_2 P_2(\cos\Theta), \tag{22}$$

where the $\tilde{\omega}_i$'s are constants and the $P_i(\cos\Theta)$'s are Legendre polynomials.

(ii) For a given particle phase function it is necessary to solve the equation of transfer for the problem of diffuse reflection giving $I(\mu, \phi; \mu_0)$, allowing for multiple scattering. This problem has been the subject of extensive investigations by Chandrasekhar (1950), whose methods are used in our discussion (see van de Hulst, 1952, for a discussion of the inade-

quacies of earlier investigations). The comparison of the theoretical values of $I(\mu, \phi; \mu_0)$ with observed *limb-darkening* results can be made at this point.

(iii) From the computed values of $I(\mu, \phi; \mu_0)$ the properties of the *total light* reflected by the planet may be determined by integration over the visible portion of the planetary disk. The necessary cubature formulae and coefficients are tabulated by Horak (1950). Letting the incident flux density be πF, the integrations give $j(\alpha)/F$, from which the geometric albedo, $p = j(0)/\pi F$, and the phase variation, $\Phi(\alpha) = j(\alpha)/j(0)$, follow. As $\Delta m(\alpha) = -2.5 \log \Phi(\alpha)$, the theoretical results can be compared with the observed phase variation, $\Delta m(\alpha)$.

(iv) The final step is the determination of the *Bond albedo*. Since $A = p \times q$, A is found from p and the integral,

$$q = 2\int_0^{\pi} \Phi(\alpha) \sin \alpha \, d\alpha .$$

8.5 Limb Darkening, Optically Thick Atmospheres

8.51. *Theory.*—Though the principal interest in the theory of diffuse reflection relates to the total light of the planet and not to local studies of planetary detail, the determination of $I(\mu, \phi; \mu_0)$ is a necessary step in the computations, and comparison of the theoretical discussion of limb-darkening observations may give the only clue to the actual form of the particle phase function.

The limb-darkening-curves for different particle phase functions at full phase can be approximated by the simple formula

$$I(\mu) = I(1.0)\,[1 - b(1 - \mu) + c(1 - \mu)^2], \text{ valid for } 0 \leqslant \mu \leqslant 1 . \quad (23)$$

Observationally, it is very difficult to obtain reliable observations beyond $r/R = 0.9$, which includes the range of $0.4 < \mu < 1.0$. Therefore, it is very difficult to determine both b and c from observations, and normally only the coefficient b is obtained, on the assumption that c is zero; this is often called the "limb-darkening coefficient." It appears that, instead of comparing limb-darkening coefficients, it is preferable to consider *the intensity at the characteristic point*, $\mu = 0.5$ or $r/R = 0.866$, and define *the ratio* $x = 2\,I(0.5)/I(1.0)$. This ratio has the important property that, to the extent that $I(\mu)$ can be represented by the second-degree expression given above, $p = j(0)/\pi F = I(1.0)(1 + 2x)/3$. As the quantity p is more easily determined from observations than is $I(1, 0)$, we have used p and x to classify the results for a number of theoretical limb-darkening-curves listed in Table 23. For Lambert's law, $p = 2\lambda_0/3$ and $x = 1.00$.

The results tabulated in Table 23 show the following characteristics.

a) For a given form of the particle phase function, $f(\cos\Theta)$, the values of p decrease rapidly with the *particle albedo*, $\tilde{\omega}_0$. At the same time, x increases, indicating that the limb darkening becomes less pronounced.

b) For a given value of $\tilde{\omega}_0$, the values of p and x increase as the anisotropy of the particle phase functions changes from forward to backward scattering.

c) The values of p and x found for Rayleigh scattering, which properly allows for polarization, show small but significant differences from the results obtained with the Rayleigh phase function. Although the latter has often been employed in the past, only the former has any physical significance.

d) The values of p and x found for Rayleigh scattering (and also for the Rayleigh phase function approximation) appear to be essentially the result of the backward-scattering component.

8.52. *Limb darkening of the major planets.*—The values of the geometric

TABLE 23

THEORETICAL LIMB-DARKENING PARAMETERS

	p	x
Isotropic scattering and $\varpi_0 = 1.000$	0.690	0.96
0.999	.636	1.01
0.995	.575	1.07
0.990	.534	1.12
0.985	.505	1.15
0.980	.482	1.18
0.975	.462	1.20
0.950	.392	1.30
0.925	.345	1.36
0.900	.310	1.41
0.850	.257	1.50
Anisotropic scattering, with $1+\cos\Theta$	.611	0.73
$1+0.6\cos\Theta$	.647	0.84
$1+0.2\cos\Theta$	.677	0.92
$1-0.2\cos\Theta$	.702	0.99
$1-0.6\cos\Theta$	.723	1.05
$1-\cos\Theta$	.742	1.11
$0.975\,(1+\cos\Theta)$	.343	0.89
$0.975\,(1+0.6\cos\Theta)$	.398	1.05
$0.975\,(1+0.2\cos\Theta)$	.442	1.16
$0.975\,(1-0.2\cos\Theta)$	.480	1.24
$0.975\,(1-0.6\cos\Theta)$	.512	1.31
$0.975\,(1-\cos\Theta)$	.539	1.37
Rayleigh scattering	.798	1.09
Rayleigh phase function or $3\,(1+\cos^2\Theta)/4$	0.752	1.05

albedos, p, of the major planets are given in Table 20, and it is seen that none approaches the value of 0.80 given by Rayleigh scattering or the value of 0.69 given by isotropic scattering with $\tilde{\omega}_0 = 1.0$, indicating that we must consider the cases of non-conservative scattering, i.e., $\tilde{\omega}_0$ less than 1.

The values of x determined from the observed limb-darkening-curves are uncertain for the following reasons:

a) The photometric problem of measuring the variation of intensity over the small disk of a planet photograph only a few millimeters in diameter is complicated by atmospheric seeing effects and photographic effects that are difficult to allow for.

b) The apparent surface of the planet shows bands and/or spots. Therefore, it is necessary to combine many limb-darkening-curves in order to obtain a representative mean that can be compared with theory.

For Jupiter and Saturn the measures by Barabaschev and Semejkin (1933, 1934) and Sharonov (1939, 1940) indicate that x is less than 1—say 0.8—in the red region and increases to about 1.2 in the blue region of the spectrum. Kuiper's measures of Jupiter at 3500 A (quoted by van de Hulst, 1952, p. 100) indicate that x increases to 1.52, while in the infrared, at 13000 and 16000 A, x is a little less than 1.

The difficulties of observation increase for the more distant planets, Uranus and Neptune. However, Richardson (1955) has observed Uranus with the 100-inch reflector and finds that the intensity variation across the disk is similar to that of Jupiter.

The ultraviolet results for Jupiter, $p(u) = 0.25$, $x = 1.52$, can be interpreted as being due to isotropic scattering with albedo $\tilde{\omega}_0 = 0.85$. However, isotropic scattering cannot explain the results in the blue, visual, and red regions, as the computed values of x are too large for the corresponding values of p. In order to obtain agreement with the observed measures, it appears that one must postulate a forward-scattering particle phase function, a simple form of which might be $f(\cos\Theta) = \tilde{\omega}_0(1 + a\cos\Theta)$.

This case was first examined by Horak (1950), at which time the necessary auxiliary functions had not yet been computed (Appendix I), and approximations were obtained by interpolation between $f(\cos\Theta) = \tilde{\omega}_0$ and $f(\cos\Theta) = \tilde{\omega}_0(1 + \cos\Theta)$. Using this method, he suggests that, for the visual region, Saturn's limb-darkening-curves can be explained by $f(\cos\Theta) = 0.985\,(1 + 0.9\cos\Theta)$, for which $p_V = 0.40$, $x = 0.91$; similarly in the blue region, $f(\cos\Theta) = 0.925\,(1 + 0.65\cos\Theta)$ and $p_V = 0.27$, $x = 1.18$.

Using the same method but giving less weight to the measures near the

limb, we obtain a less extreme form of scattering function, $f(\cos\Theta) = 0.98\,(1 + 0.6\cos\Theta)$, for which $p = 0.43, x = 1.01$, to explain the observations of Jupiter and Saturn in the visual region.

It is recognized that the simple adopted form of anisotropic scattering is only a mathematical simplification; but the limited accuracy of the observed limb-darkening-curves does not at present appear to justify an extension of the theoretical investigation to more complicated forms for $f(\cos\Theta)$.

8.6. Variation with Solar Phase Angles and the Bond Albedo

The integrated or total light, diffusely reflected toward the earth by the planet at a given phase angle α, is

$$j(\alpha) = \int I(\mu, \phi; \mu_0)\,\mu dS\,. \tag{24}$$

TABLE 24

Theoretical Phase Variations, $\Phi(\alpha)$

α	Rayleigh Scattering	Isotropic Scattering		Forward Scattering		Lambert's Law
		$\varpi_0 = 1.00$	$\varpi_0 = 0.95$	$0.975\,(1+0.5\cos\Theta)$	$0.985\,(1+0.9\cos\Theta)$	
0°	1.00	1.00	1.00	1.00	1.00	1.000
20	0.91	0.94	0.93	0.95	0.96	0.944
40	0.71	0.78	0.79	0.82	0.84	0.800
50	0.59	0.69	0.70	0.74	0.77	0.708
60	0.48	0.58	0.60	0.65	0.68	0.609
80	0.31	0.39	0.42	0.46	0.51	0.410
100	0.18	0.22	0.25	0.29	0.33	0.236
120	0.091	0.106	0.13	0.16	0.18	0.109
140	0.037	0.037	0.049	0.062	0.070	0.034
160	0.009	0.006	0.010	0.012	0.016	0.006
180°	0.000	0.000	0.000	0.000	0.000	0.000
q	1.25	1.45	1.52	1.65	1.77	1.50
$q/\Phi(50°)$	2.11	2.12	2.19	2.24	2.30	2.12

At full phase, $\alpha = 0°$, and we obtain $j(0)/\pi F = p$, already considered. For other phase angles the brightness is expressed in terms of the brightness at full phase, or $\Phi(\alpha) = j(\alpha)/j(0)$. From $\Phi(\alpha)$ we compute the integral

$$q = 2\int_0^\pi \Phi(\alpha)\sin\alpha\, d\alpha$$

and obtain the Bond albedo, $A = p \times q$.

The values of $j(\alpha)/F$ for several different particle phase functions have been computed by Horak, from which we have obtained the values of $\Phi(\alpha)$ tabulated in Table 24; the results for Lambert's law have been taken

from Schönberg (1929). The last two lines of the table give the integral q and the ratio q/Φ (50°). The latter ratio was found to be about 2.17 from the observed phase-curves of the moon and terrestrial planets; it appears that the ratio increases slightly with the brightness at phase angle 50°.

From the examples listed in Table 24 it is seen that Rayleigh scattering gives the most rapid brightness decrease with phase angle, while the forward-scattering phase functions show the slowest decrease. For all the phase functions considered, the decrease in brightness over the first few degrees is very small; for example, Talley and Horak's (1956) accurate integration for isotropic scattering ($\tilde{\omega}_0 = 1.0$) gives Δm (10°) $= -2.5$ log

TABLE 25

THEORETICAL ALBEDO PARAMETERS, p, q, AND A

	p	q	A
Isotropic scattering and $\varpi_0 = 1.000$	0.690	1.45	1.00
0.975	.462	1.52	0.70
0.950	.392	1.52	0.60
Anisotropic scattering with $1+\cos\Theta$	.611	1.64	1.00
$1+0.6\cos\Theta$	.647	1.55	1.00
$1+0.2\cos\Theta$	.677	1.48	1.00
$1-0.2\cos\Theta$	.702	1.42	1.00
$1-0.6\cos\Theta$	.723	1.38	1.00
$1-\cos\Theta$	.742	1.35	1.00
$0.975\,(1+0.5\cos\Theta)$	.41	1.65	0.67
$0.985\,(1+0.9\cos\Theta)$	.40	1.77	0.71
Rayleigh scattering	.798	1.25	1.00
Rayleigh phase function, $\varpi_0=1.000$	.752	1.33	1.00
$3\varpi_0(1+\cos^2\Theta)/4$, $\varpi_0=0.975$	.52	1.32	0.69
$3\varpi_0(1+\cos^2\Theta)/4$, $\varpi_0=0.950$	0.45	1.33	0.60

Φ (10°) $=$ 0.020 mag., so that a linear phase coefficient of the order of only 0.002 mag/degree would be expected. This is the order of magnitude obtained empirically for Uranus; it suggests that the higher values found for Jupiter are due to irregularities, such as spots.

Using q as a parameter to characterize the variation with solar phase angle, we may derive values of $q = 1/p$ for the cases of conservative scattering discussed earlier. The results are collected in Table 25. From these we see that q increases slightly with decreasing particle albedo, while the asymmetry of the particle phase function introduces considerable changes, in the sense that forward-scattering functions have the larger q's. The low values of q for Rayleigh scattering (and for the Rayleigh phase-function

approximation) can be attributed to the backward-scattering component. The values listed for $f(\cos\Theta) = \tilde{\omega}_0[\frac{3}{4}(1 + \cos^2\Theta)]$ are based on approximations discussed in the next section.

8.61. *The phase variation of Venus.*—The planet Venus can be observed over a large range in phase angle, and the variation in brightness is well determined by Danjon's (1949) measures. From the observed variation one finds that the integral q is only 1.30, which, combined with $p = 0.55$, gives a Bond albedo in the visual region of 0.71. The low value of q indicates that the variation with phase angle must be similar to that found for Rayleigh scattering, implying an anisotropic particle phase function with

TABLE 26

OBSERVED AND THEORETICAL PHASE VARIATION OF VENUS

α	Observed (Danjon)	Rayleigh Scattering	$0.975\ [\frac{3}{4}(1+\cos^2\Theta)]$
0°	1.00	1.00	1.00
20	0.91	0.91	0.92
40	0.71	0.71	0.73
60	0.49	0.48	0.52
80	0.31	0.31	0.33
100	0.18	0.18	0.20
120	0.107	0.091	0.102
140	0.062	0.037	0.042
160	0.036	0.009	0.009
180°	0.023	0.000	0.000
p	0.548	0.798	0.52
q	1.296	1.33	1.32
A	0.71	1.00	0.69

a strong backward component. We have tabulated the values of $\Phi(\alpha)$ as defined by Danjon's results in the second column of Table 26, along with the values given by Rayleigh scattering. It is seen that the agreement is quite good up to about phase angle 120° but that there is an excess observed brightness for larger phase angles. The value given for 180° results from an extrapolation of Danjon's measures from his upper limit of 171°, and indicates that the excess is about 2.3 per cent. It is well known that Venus can be observed as an annulus near inferior conjunction, the ring being considerably brighter than the sky in its neighborhood. This excess brightness is attributed to light diffused around the edge of the planet by the atmosphere—it is probable that the excess brightness at large phase angles over the Rayleigh values can be accounted for in the same manner.

As the Bond albedo is less than unity, we must introduce a particle albedo $\tilde{\omega}_0$, less than unity, and we are led to investigate the possibility that

the particle phase function has the form $f(\cos \Theta) = \tilde{\omega}_0[\frac{3}{4}(1 + \cos^2 \Theta)]$ which would reduce p and at the same time presumably have a phase variation similar to that of Rayleigh scattering. The accurate solution for a phase function of this form has not been attempted. However, Chandrasekhar (1950, p. 146) has pointed out that the effects of higher-order scattering for the Rayleigh phase function and for isotropic scattering are very similar. Accordingly, we have made the approximation that first-order scattering obeys our modified Rayleigh phase function, while the higher-order scattering is that given by isotropic scattering with the same albedo. This seems to be a rather good approximation for cases where the deviation from isotropy is small, but it becomes increasingly poorer as the phase function becomes more and more asymmetrical.

The solutions for this approximation are summarized in the last section of Table 25, and the computed phase variation for $\tilde{\omega}_0 = 0.975$ is given in the last column of Table 26. Although this is only an approximate solution and must be confirmed by accurate computations, it appears that an exact solution will probably explain the general features of the photometric behavior of Venus.

Horak (1950), who investigated the problem of Venus, suggested that isotropic scattering with $\tilde{\omega}_0 = 0.95$ would represent the phase variation for angles less than 130° as well as the limb-darkening measures. In regard to the phase variations, the difference between his computed q of 1.52 and the observed value is considerable, while Minnaert (1946) has shown that the limb-darkening measures do not satisfy the reciprocity principle and therefore cannot be represented by any of the simple theoretical cases considered here.

8.62. *The adopted values of q for the major planets.*—It appears that three courses are open in the selection of an appropriate value of q for use in albedo determinations of the major planets. First, one might adopt the value of $q = 1.30$ found for Venus, on the premise that both Venus and the major planets possess optically thick atmospheres. Second, one might assume that the major planets are covered by a cloud surface that reflects light according to Lambert's law, which would be in rough agreement with the limb-darkening results, for which x varies from, say, 0.8 to 1.2. This is the course adopted by Russell (1916*b*), who takes $q = 1.50$.

The third alternative is to assume that the major planets have optically thick atmospheres and to obtain from the limb-darkening measures the result that the particle phase function must have a forward component which decreases with wave length, becoming nearly isotropic in the ultraviolet. This is the course adopted by Horak (Sec. 8.5); his particle phase

functions lead to $q = 1.77$ in the visual region and about 1.65 in the blue region. We are inclined to adopt a somewhat less extreme particle phase function, which gives less weight to the observed darkening results near the limb. We have adopted $q = 1.65$ for the visual, $q = 1.60$ for the blue, and $q = 1.55$ for the ultraviolet measures.

For a definitive estimate of the albedos of the outer planets, it is imperative that mean limb-darkening observations of high precision be obtained in the various wave-length regions. These, combined with more extensive theoretical investigations involving different forms of the particle phase function, should lead to considerably better values of the albedos than those given here.

One aspect that must be kept in mind is that the observations of the major planets can be made only near full phase, and it is possible that two radically different particle phase functions may lead to the same law of darkening. A simple example is that afforded by

$$f(\cos \Theta) = 0.925\,(1 + \cos \Theta),$$

which leads to a law of darkening that agrees with Lambert's law over the whole disk to within a fraction of a per cent. It is probable that q for this phase function is of the order of 1.7 instead of the Lambert value of 1.5.

8.7. Planet with No Atmosphere

The planet Mercury and the moon show very similar variations with solar phase angle, and this variation deviates markedly from any known law of diffuse reflection—for example, Lambert's law or the Lommel-Seeliger law. As the photometry of the moon has been reviewed by Minnaert in chapter 6, we limit our remarks to an attempt to discover an empirical law of reflection from the lunar observations.

We have examined Bennett's (1938) observations of the variation in brightness of a number of lunar positions with phase angle in an effort to find an interpolation formula that would represent his observations of relative brightness, h/h_0, as a function of phase angle. An early investigation by Öpik (1924) led him to adopt the empirical law,

$$\frac{h}{h_0} = C\,(\cos i)^k, \tag{25}$$

where h_0 is the brightness of an area at full phase and C and k are constants that depend on α only. Minnaert (1941, p. 409) pointed out that this relation did not satisfy the reciprocity principle and suggested that it might be modified to

$$\frac{h}{h_0} = C\,(\cos i)^k\,(\cos \epsilon)^{k-1}, \tag{26}$$

where again C and k depend on α only. The value of k is found from measures made on the same photographic plate, but the constant C depends on the adopted zero point of the plate, which in Bennett's observations was adjusted to fit Russell's (1916*a*) lunar phase-curve.

From Bennett's data it appears that, for phase angles greater than 90°, k is nearly equal to 1.0, so that Minnaert's law reduces to Lambert's law in this case. At full moon we take $k = 0.5$, to agree with the observed fact that there is no limb darkening at this phase. For intermediate phase angles we have obtained the value of C and k given in Table 27. A check of a number of individual areas shows that our interpolation formula is quite satisfactory for both maria and terrae as was to be expected from Bennett's own discussion (Fig. 18).

TABLE 27

CONSTANTS DERIVED FOR MINNAERT'S LAW OF REFLECTION
(Bennett's Data)

α	C	k	α	C	k
0°...	1.00	0.50	50°...	0.54	0.82
10...	0.88	0.58	60....	0.51	0.87
20...	0.78	0.64	70....	0.50	0.92
30...	0.69	0.70	80....	0.50	0.96
40°...	0.61	0.76	90°...	0.50	1.00

The integration of our interpolation formula over the disk at any given phase angle should reproduce Russell's mean light-curve for the moon, provided that we assume that the distribution of light and dark areas is uniform over the disk. The fact that Rougier's curve shows little difference between increasing and decreasing phase angles indicates that this is a quite good approximation, in spite of the fact that the fraction of the illuminated surface covered by maria varies considerably (Danjon, 1933). For phase angles greater than 90°, Rougier's curve would give $C = 0.363$ instead of 0.50, and it is a simple matter to compare with Rougier's curve in this region as well. The comparison of observed and theoretical variations given in Table 28 appears to be satisfactory, although slight adjustment of the constants might bring them into better agreement.

Figure 19, showing the form of the law of reflection for different angles of incidence, is comparable to that given by Minnaert in chapter 6, Figure 9.

8.8. PLANET WITH AN OPTICALLY THIN ATMOSPHERE

The case of an optically thin atmosphere overlying the surface of a planet will, in the absence of clouds, apply to the earth, where in the visual

TABLE 28

OBSERVED AND COMPUTED PHASE VARIATION OF THE MOON

α	Russell	Computed	Rougier	Computed
0°	1.00	1.00	1.00	1.00
20	0.65	0.65	.....	.....
40	0.41	0.39	.....	.....
60	0.26	0.23	.....	.....
80	0.15	0.14	.....	.....
100	0.075	0.079	0.057	0.057
120	0.031	0.036	0.026	0.026
140	0.010	0.012	0.009	0.008
150°	0.004	0.005	0.005	0.004

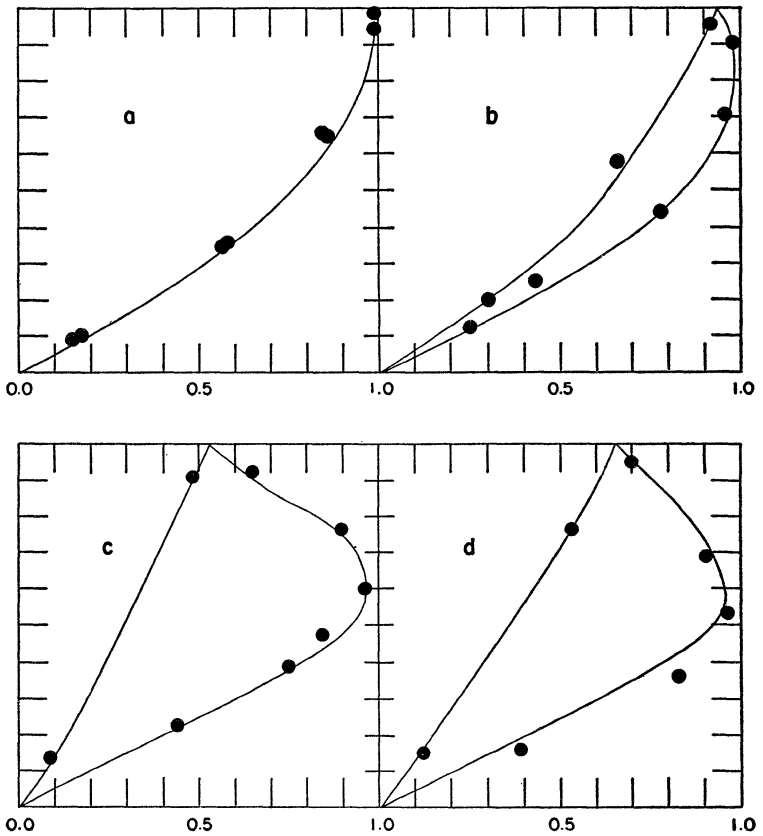

FIG. 18.—Comparison of Bennett's lunar observations with Minnaert's empirical law of diffuse reflection; *abscissae:* cos i; *ordinates:* h/h_0. (*a*) Centrally located maria; (*b*) terrae; (*c*) maria near limb; (*d*) dark crater floor near limb.

region $\tau = 0.15$ and increases to about 0.5 at 3540 A, and also to Mars, where the optical thickness is about one-third that of the earth. The case will also apply to a thin atmosphere overlying a cloud surface, such as might be encountered for Venus or the major planets.

The exact solutions for the emergent intensity are given by Chandrasekhar (1950, p. 270) for the special case of a ground reflecting according to Lambert's law with an albedo λ_0. The necessary functions for numerical application of the formulae have been computed for isotropic scattering and Rayleigh scattering (see Appendix I, this chapter).

The possible application to Venus and the major planets is suggested by the fact that small particles and molecules will not be thoroughly mixed; instead, the particles will tend to settle in the atmosphere. The "atmosphere" will then consist of molecules, which obey the Rayleigh scattering law, and will largely account for the observed polarization. It is assumed that below this "atmosphere" a cloud surface exists which reflects light according to Lambert's law.

Assuming $\lambda_0 = 0.60$ and a thin isotropic atmosphere with $\tilde{\omega}_0 = 1.0$, we find the values of p and x given in Table 29. The addition of an optically

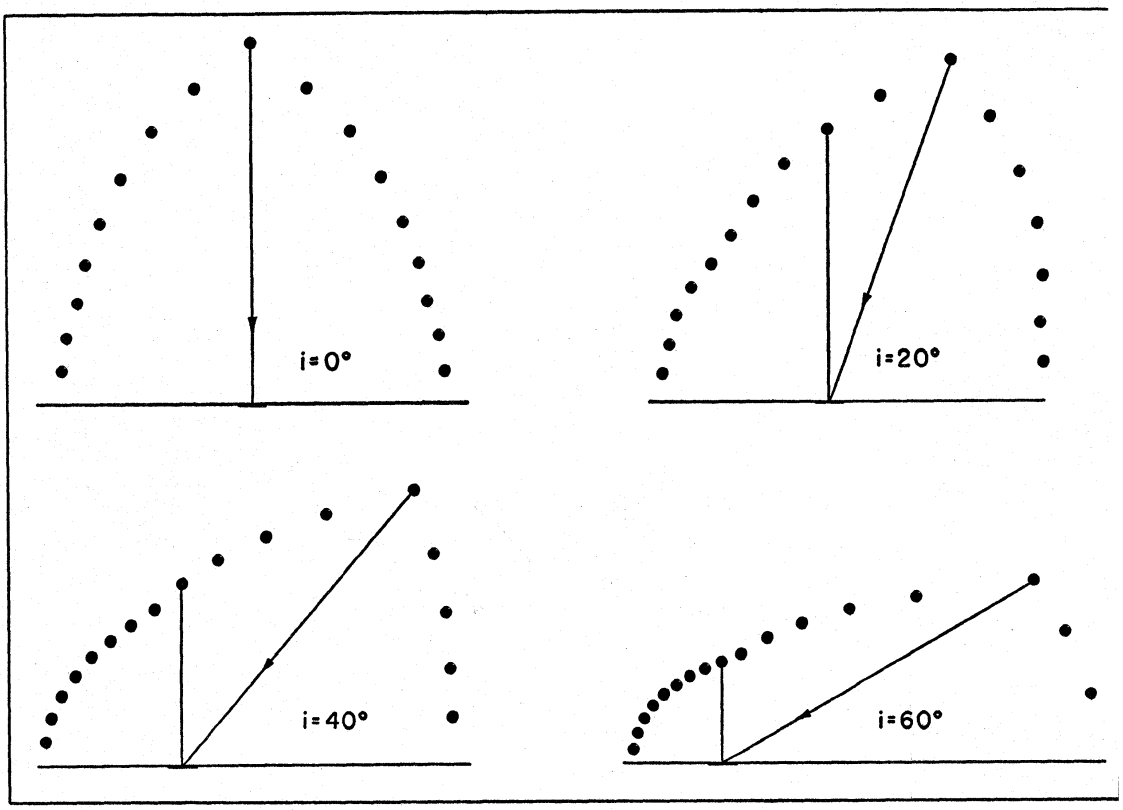

FIG. 19.—Indicatrices for Minnaert's law of diffuse reflection for various angles of incidence

thin atmosphere to a Lambert sphere appears to increase p only slightly; but the limb darkening decreases, because of the increased brightness near the limb, where the effective optical thickness becomes large because of the secant factor.

From an examination of a number of combinations of λ_0, $\tilde{\omega}_0$, and τ it does not appear that the Lambert "cloud" model can give the small values of x observed for the major planets in the visual and red regions. It appears that a model consisting of an optically thin layer of molecules obeying Rayleigh scattering, overlying a semi-infinite atmosphere of particles with a backward-scattering phase function, would be required to satisfy both the observed limb darkening and Lyot's polarization-curve.

For the case of a thin atmosphere overlying the solid surface of the planet, which is assumed to obey Lambert's law with a low albedo, the brightening at the limb by the atmospheric contribution modifies the results considerably. The limb darkening computed for a Lambert sphere with $\lambda_0 = 0.10$ and a thin atmosphere, scattering isotropically with $\tilde{\omega}_0 = 0.95$, is shown in Table 30. The influence of the atmosphere is most impor-

TABLE 29

LIMB DARKENING FOR OPTICALLY THIN ATMOSPHERE AND LAMBERT GROUND, $\varpi_0 = 1.0$, $\lambda_0 = 0.6$

τ	p	x	τ	p	x
0.00...	0.40	1.00	0.50....	0.44	1.16
.10...	.41	1.03	1.00....	0.46	1.22
0.25...	0.42	1.09			

TABLE 30

LIMB DARKENING FOR OPTICALLY THIN ATMOSPHERE AND LAMBERT GROUND, $\lambda_0 = 0.10$, $\varpi_0 = 0.95$

μ	r/R	$I(\tau=0.00)$	$I(\tau=0.05)$	$I(\tau=0.25)$	$I(\tau=1.00)$
1.0...	0.00	0.100	0.108	0.144	0.277
0.8...	0.60	0.080	0.094	0.136	0.274
0.6...	0.80	0.060	0.078	0.134	0.266
0.4...	0.92	0.040	0.065	0.140	0.245
0.3...	0.95	0.030	0.064	0.147	0.226
0.2...	0.98	0.020	0.068	0.156	0.199
0.1...	0.995	0.010	0.089	0.154	0.165
0.0...	1.00	0.000	0.119	0.119	0.119
p.....	.....	0.067	0.085	0.139	0.261
x.....	.....	1.00	1.31	1.89	1.86

tant very close to the limb but is still appreciable in the observable region, $\mu = 1.0$–0.4.

If an arbitrary law of diffuse reflection for the ground is substituted for Lambert's law, an exact solution appears to be extremely difficult to compute; but for small optical thickness and ground albedo the emergent intensity can be estimated with considerable accuracy. We have used the empirical law of diffuse reflection derived from the lunar observations (Sec. 8.7), which we shall denote as the "lunar law," and an isotropic scattering atmosphere with $\tilde{\omega}_0 = 1.00$ and $\lambda_0 = 0.10$. The albedo of the "ground" was adjusted to give a total albedo of 0.14. This result is compared in Table 31 with the solution for Lambert's law with $\lambda_0 = 0.067$ and the same atmosphere, which leads to the same Bond albedo. The phase variations of the earth as derived by Danjon (Vol. **2**, chap. 15) and of Mars are also tabulated for comparison.

TABLE 31

PHASE VARIATION OF PLANET WITH OPTICALLY THIN ATMOSPHERE

α	Lambert Ground	"Lunar" Ground	Earth Observed	Mars Observed
0°	1.00	1.00	1.00	1.00
20	0.93	0.76	0.78	0.74
40	0.78	0.55	0.59	0.55
60	0.63	0.41	0.42	.....
80	0.46	0.29	0.27	.....
100	0.33	0.22	0.16	.....
120	0.21	0.13	0.09	.....
140	0.10	0.06	0.04	.....
160°	0.03	0.02	0.02	.....
p	0.083	0.117	0.366	0.144
q	1.70	1.16	1.095	1.04
A	0.14	0.14	0.40	0.15

It is seen that the observed phase variation of the earth is more nearly like that computed with the lunar law of reflection than that computed with Lambert's law. Although it is not reasonable to assume that the surface of the earth reflects like the surface of the moon, it is possible that the Martian surface with no open water reflects light in a manner quite similar to the moon and Mercury; it should be remembered that the photometric properties of the moon are determined by its small-scale irregularities and not by the visible mountains. It is seen that the Mars observations are well represented by the model.

9. SATELLITE ECLIPSES AND OCCULTATIONS OF STARS

9.1. Observations of Eclipses of Jupiter's Satellites

Photometric observations of the eclipses of Jupiter's satellites were initiated at the Harvard Observatory in 1878 by Pickering (1907), and the results for the times of mid-eclipse were made the basis of the *Tables of the Four Great Satellites of Jupiter* by Sampson (1910). Photographic photometry of eclipse light-curves was carried out by King (1917); he found that the scattered light from Jupiter produced an appreciable sky background which was difficult to correct for in the reductions.

In 1950 Kuiper made observations of the disappearances of Jupiter I and II with the photoelectric photometer at the Cassegrain focus of the 82-inch McDonald reflector, and in 1954 Kuiper and Harris obtained at least one light-curve of each of the satellites as they went into eclipse. The observing procedure was to start observations of the satellite approximately 10 minutes before predicted time of first contact and then adjust the rate of the telescope drive so that it followed the satellite. Although this adjustment could be made with considerable accuracy, the observations were made through a diaphragm of diameter 12 seconds of arc to insure that guiding errors would be negligible. The bright sky background was allowed for by making measurements on regions close to the satellite and interpolating for the position of the object. At the end of the run when the satellite had diminished by about 9.0 mag. (or a factor of 4000 in brightness), the sky deflection was given directly.

The measurements were made through the yellow filter, and a continuous eclipse-curve was traced out on the recorder, the record being interrupted only to check the centering or to change the amplification of the signal. The traces were then reduced by taking readings at equal time intervals sufficiently far apart that they would be essentially independent—the time constant of the amplifier being 1 second.

Measurements made before first contact indicate that the accidental error is about ± 0.3 per cent for one point. During the intervals before the start of the eclipses all four satellites remained constant in brightness within the error of measurement.

Table 32 gives a summary of the eclipses observed at the McDonald Observatory. The observed time of mid-eclipse is taken to be the time when the brightness, B, drops from the adopted value of 100.0 outside eclipse to 50.0. The times should be accurate to better than ± 2 seconds. The predicted times of mid-eclipse, taken from the *American Ephemeris*, yield the residuals, $O - C$, given in the last column.

TABLE 32

OBSERVED U.T. OF MID-ECLIPSE

Ec. D. I.....	1950	Aug. 11^d 8^{h}26^{m}22^s	−1^{m}2
	1954	Nov. 19 9 56 38	−1.2
	1954	Nov. 26 11 50 16	−1.2
Ec. D. II.....	1950	July 28 9 52 51	−0.9
	1954	Nov. 16 10 34 14	−0.9
Ec. D. III.....	1954	Nov. 19 8 21 02	+0.2
	1954	Nov. 26 12 19 12	+0.3
Ec. D. IV.....	1954	Dec. 31 8 54 17	−2.0

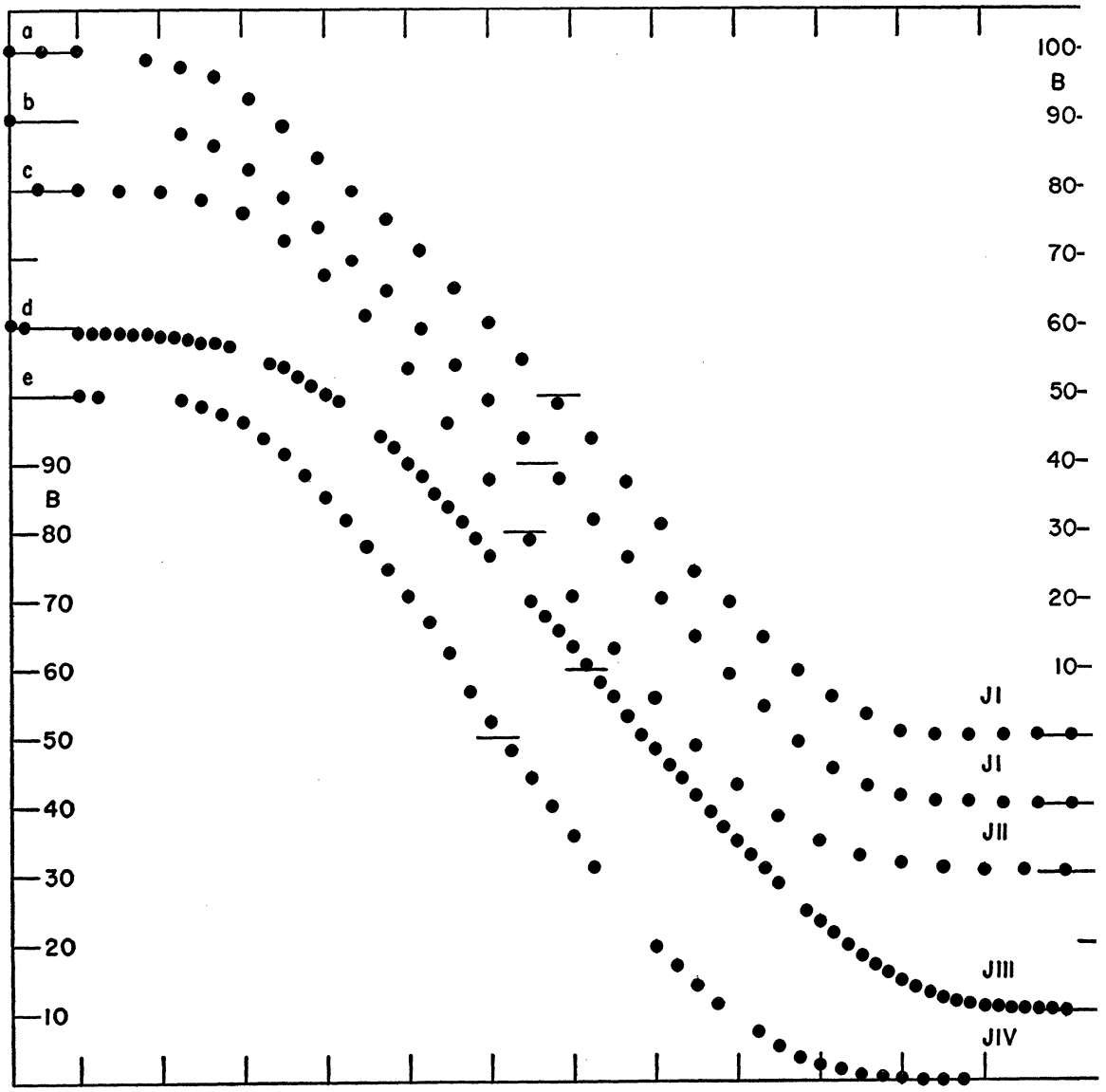

FIG. 20.—Eclipses of Jupiter's satellites on an intensity scale. (*a* and *b*) Jupiter I; (*c*) Jupiter II; (*d*) Jupite III; (*e*) Jupiter IV. The measures are listed in Tables 33–37. Short horizontal lines near center indicate half-in tensity points.

The observed light-curves for the eclipses which were considered the most reliable are given in detail in Tables 33–37, and the observations are plotted in Figure 20, *a–e*, on an intensity scale. The light-curves of I and III observed on November 26 are also plotted on a magnitude scale, in Figure 21, *a–b*.

9.2. Theoretical Eclipse Light-Curves

Sampson (1909) has computed theoretical light-curves which were used in the reduction of the Harvard series of eclipses. As his calculated curves are not quite accurate enough for use in comparisons with the McDonald data, we have redetermined theoretical curves based on the following assumptions. For any point on the satellite's disk, during the progress of the eclipse, the limb of Jupiter will cut off a portion of the sun's disk, and the

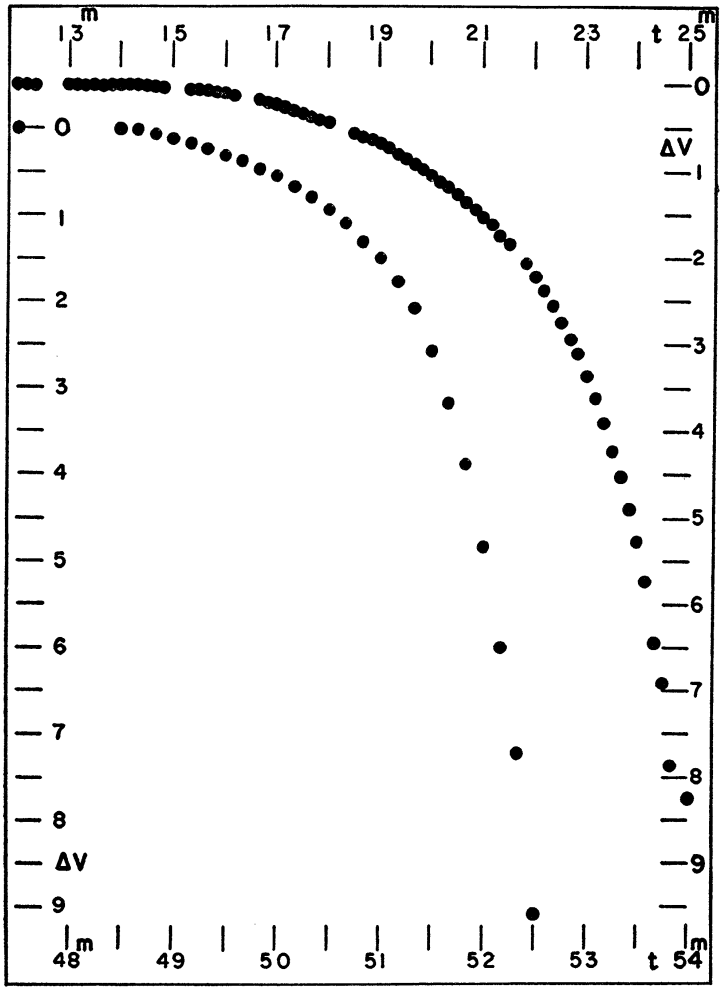

Fig. 21.—Observations of the eclipse of Jupiter III (*upper curve*) and of Jupiter I made on November 26, 1954, plotted on a magnitude scale.

illumination of this point is given by the brightness of the unobscured portion of the sun. If it be assumed that the brightness of the point is proportional to the illumination, integration of the illumination over all points on the disk will give for each epoch the integrated brightness of the satellite. In our calculations we have assumed a limb-darkening coefficient for the sun of 0.6 but assumed that there is no limb darkening on the satellite. In the case of Jupiter IV the deviation of the projected limb of Jupiter on the sun from a straight line necessitates a small correction, while for the other satellites the deviation is negligible. Also, in the cases of Jupiter III and IV, the variable motion of the satellite during the eclipse has been allowed for by using the results given by Sampson (1910).

The diameters of the satellites used in the calculations (expressed in terms of the earth's diameter) are as follows: I, 0.255; II, 0.226; III, 0.394; and IV, 0.350; these values are essentially the values listed by Kuiper in chapter 4.

The residuals, $O - C$, for each of the observed points are given in Tables 33–37, and these residuals are plotted against phase in Figure 22, *a–e*. The diameter of the circles corresponds to 0.4 units in B, slightly larger than the estimated accuracy of the measures. It is apparent that all the curves of residuals show systematic trends, the residual at mid-eclipse being arbitrarily adjusted to zero.

Sampson in his discussion enumerated several reasons why the observed and theoretical curves might not agree; some of these will be examined here.

(i) Refraction in Jupiter's atmosphere. The effect of refraction in Jupiter's atmosphere is discussed in some detail in Section 9.3. However, it appears that, for a reasonable assumption concerning the refraction and over the range in brightness which our observations cover, the effect is similar to a very small change in the satellite radius. For Jupiter IV, where refraction plays the most important role, the correction never amounts to more than 0.3 unit.

(ii) The adopted satellite diameter may not be appropriate. The measured diameters of the satellites used in our computations are about 4 per cent smaller than the "photometric" diameters adopted by Sampson, which gave the best fit for the Harvard eclipse observations. The effect of increasing the adopted diameter of I by 5 and 14 per cent reduces the residuals, $O - C$, for the November 26 curve to those shown in Figure 23, *a* and *b*. It appears that the McDonald observations of all the satellites are also better represented by "photometric" diameters that are larger than the measured diameters.

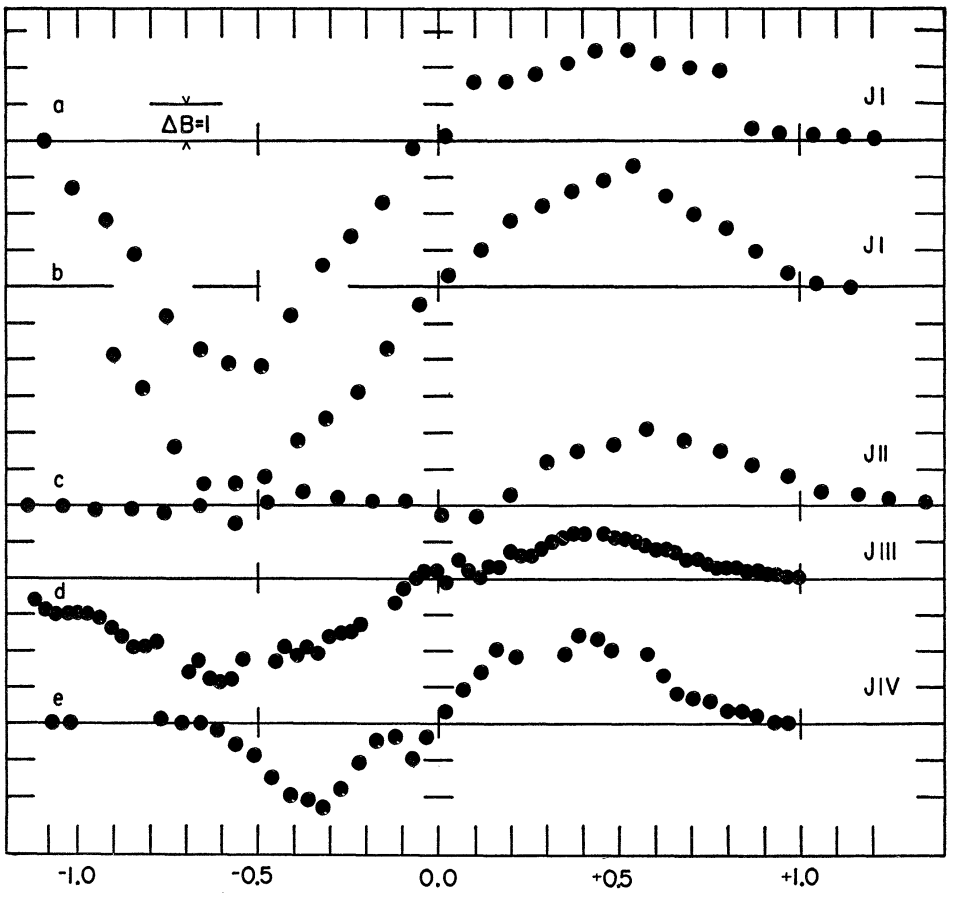

FIG. 22.—Differences (observed-theoretical) for eclipse-curves. *Abscissae:* phase measured from mid-eclipse; *ordinates:* marked at intervals of $B = 1.0$. (*a* and *b*) Jupiter I; (*c*) Jupiter II; (*d*) Jupiter III; (*e*) Jupiter IV.

TABLE 33

ECLIPSE DISAPPEARANCE OF JUPITER I ON NOVEMBER 19, 1954

U.T.	*B*	*O*−*C*	U.T.	*B*	*O*−*C*
09:54:00	100.0	0.0	09:56:40	48.8	+0.1
10	100.0	0.0	50	43.7	+1.6
20	100.0	0.0	57:00	37.2	+1.6
30	.....	.....	10	31.1	+1.8
40	98.7	−1.3	20	25.3	+2.1
50	97.7	−2.2	30	19.9	+2.5
55:00	96.2	−3.1	40	14.6	+2.5
10	93.0	−4.8	50	9.6	+2.1
20	89.2	−5.7	58:00	5.9	+2.0
30	84.7	−6.1	10	3.4	+1.9
40	79.8	−6.2	20	0.6	+0.3
50	75.6	−4.8	30	0.2	+0.2
56:00	71.1	−3.4	40	0.15	+0.15
10	65.8	−2.6	50	0.1	+0.1
20	60.3	−1.7	59:00	0.1	+0.1
30	55.2	−0.2	10	0.0	0.0

(iii) Non-uniform surface brightness of the satellites. In the simple model for the satellites considered above, we assume that the brightness of a surface element is proportional to the illumination incident upon it. If, instead, we adopt a brightness distribution over the satellite disk corresponding to the empirical law of diffuse reflection found for the moon at phase angle 10° (Sec. 8.7), then the differences between the computed curve and that for a uniform surface are positive before mid-eclipse, as shown in Figure 23, *d*. A better representation, as shown in Figure 23, *e*,

TABLE 34

ECLIPSE DISAPPEARANCE OF JUPITER I ON NOVEMBER 26, 1954

U.T.	*B*	*O*−*C*	U.T.	*B*	*O*−*C*
11:47:00	100.0	0.0	11:49:50	64.2	−2.9
10	100.0	0.0	50:00	59.2	−1.5
20	100.0	0.0	10	53.6	−0.5
30	100.0	0.0	20	47.7	+0.3
40	.....	.....	30	41.8	+1.0
50	.....	.....	40	36.1	+1.8
48:00	.....	.....	50	30.2	+2.2
10	.....	.....	51:00	24.8	+2.8
20	.....	.....	10	19.2	+2.9
30	98.0	−1.9	20	14.4	+3.3
40	96.3	−2.8	30	9.2	+2.5
50	92.9	−4.4	40	5.3	+2.0
49:00	88.8	−5.4	50	2.8	+1.6
10	84.5	−5.4	52:00	1.2	+1.0
20	79.7	−5.2	10	0.4	+0.4
30	75.1	−4.2	20	0.1	+0.1
40	69.7	−3.6	30	0.0	0.0

TABLE 35

ECLIPSE DISAPPEARANCE OF JUPITER II ON NOVEMBER 16, 1954

U.T.	*B*	*O*−*C*	U.T.	*B*	*O*−*C*
10:31:00	100.0	0.0	10:34:45	32.9	+0.3
15	100.0	.0	35:00	25.8	+1.2
30	100.0	.0	15	18.8	+1.5
45	99.9	− .1	30	12.9	+1.7
32:00	99.6	− .1	45	8.3	+2.1
15	98.5	− .2	36:00	4.7	+1.8
30	96.5	.0	15	2.5	+1.5
45	92.4	− .5	30	1.3	+1.1
33:00	87.7	+ .1	45	0.8	+0.8
15	81.6	+ .4	37:00	0.4	+0.4
30	73.9	+ .2	15	0.3	+0.3
45	66.0	+ .1	30	0.2	+0.2
34:00	57.6	+ .1	45	0.15	+0.15
15	48.9	− .3	38:00	0.1	+0.1
30	40.6	−0.1	15	0.0	0.0

may be obtained with the same law of diffuse reflection, provided that the satellite diameter is increased by 6 per cent. If ordinary limb darkening is added, a still larger satellite diameter needs to be postulated to explain the observed eclipse-curve. Such a large increase over the micrometric diameters appears ruled out.

Thus one is led to consider the effects produced by surfaces which are no longer of uniform brightness at full phase but which have large spots, somewhat like the moon. The actual presence of such spots on the Jupiter satellites follows from the fact that all of them show variations in brightness with rotational phase and that, moreover, several observers during

TABLE 36

ECLIPSE DISAPPEARANCE OF JUPITER III ON NOVEMBER 26, 1954

U.T.	*B*	*O*−*C*	U.T.	*B*	*O*−*C*
12:12:00	100.0	0.0	12:18:40	57.8	−0.3
10	100.0	0.0	50	55.6	0.0
20	100.0	0.0	19:00	53.2	+0.2
30	.....	.....	10	50.7	+0.2
40	.....	.....	20	47.9	−0.1
50	.....	.....	30	45.9	+0.5
13:00	99.4	−0.6	40	43.1	+0.2
10	99.1	−0.9	50	40.4	0.0
20	99.0	−1.0	20:00	38.2	+0.3
30	99.0	−1.0	10	35.8	+0.3
40	99.0	−1.0	20	33.8	+0.7
50	99.0	−1.0	30	31.3	+0.6
14:00	98.7	−1.3	40	28.9	+0.6
10	98.5	−1.4	50	26.8	+0.8
20	98.2	−1.6	21:00	24.8	+1.0
30	97.8	−1.9	10	22.7	+1.1
40	97.5	−1.9	20	20.6	+1.2
50	97.2	−1.8	30	18.6	+1.2
15:00	.....	.....	40	.....	.....
10	.....	.....	50	14.7	+1.2
20	94.7	−2.6	22:00	12.9	+1.1
30	94.1	−2.3	10	11.2	+1.1
40	92.6	−2.8	20	9.5	+1.0
50	91.3	−2.9	30	8.0	+0.9
16:00	90.1	−2.8	40	6.7	+0.8
10	89.2	−2.2	50	5.6	+0.8
20	.....	.....	23:00	4.5	+0.7
30	.....	.....	10	3.5	+0.5
40	83.8	−2.3	20	2.8	+0.5
50	82.2	−1.9	30	2.0	+0.4
17:00	79.9	−2.1	40	1.5	+0.3
10	77.9	−1.9	50	1.1	+0.3
20	75.5	−2.1	24:00	0.8	+0.3
30	73.7	−1.6	10	0.5	+0.2
40	71.4	−1.5	20	0.3	+0.2
50	69.0	−1.5	30	0.2	+0.1
18:00	66.8	−1.3	40	0.1	+0.1
10	.....	.....	50	0.05	+0.04
20	.....	.....	25:00	0.05	+0.05
30	59.9	−0.7	10	0.0	0.0

TABLE 37

ECLIPSE DISAPPEARANCE OF JUPITER IV ON DECEMBER 31, 1954

U.T.	*B*	*O−C*	U.T.	*B*	*O−C*
08:44:00	100.0	0.0	08:54:30	48.2	+0.3
30	100.0	0.0	55:00	43.9	+0.9
45:00	.....	.....	30	39.6	+1.4
30	.....	.....	56:00	35.5	+2.0
46:00	.....	.....	30	30.9	+1.8
30	99.2	+0.1	57:00	.....	.....
47:00	98.4	0.0	30	.....	.....
30	97.4	0.0	58:00	19.5	+1.9
48:00	95.9	−0.2	30	16.8	+2.4
30	93.8	−0.6	59:00	13.9	+2.3
49:00	91.4	−0.9	30	11.1	+2.0
30	88.4	−1.5	09:00:00	.....	.....
50:00	85.0	−2.0	30	7.1	+1.9
30	81.6	−2.1	01:00	5.1	+1.3
51:00	77.8	−2.3	30	3.4	+0.8
30	74.3	−1.8	02:00	2.4	+0.7
52:00	70.8	−1.1	30	1.6	+0.6
30	66.8	−0.5	03:00	0.9	+0.3
53:00	62.2	−0.4	30	0.6	+0.3
30	56.7	−1.0	04:00	0.3	+0.2
54:00	52.4	−0.4	30	0.0	0.0

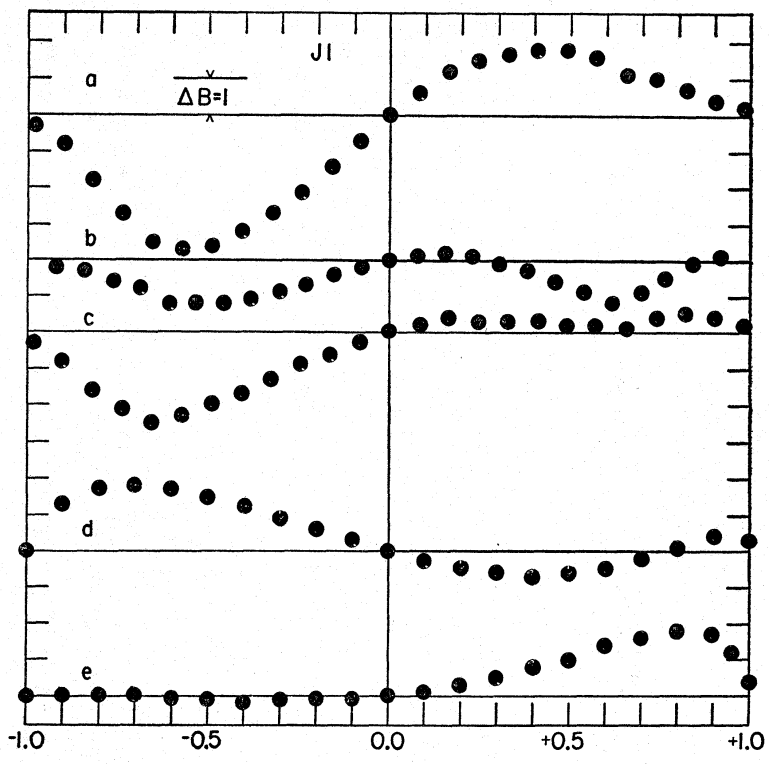

FIG. 23.—Same as Fig. 22, *b* (Jupiter I, November 26, 1954) with different radii and spots (see text for details).

the past half-century or more have noted, by direct inspection, uneven distributions of brightness over the disks (see chap. 15, Pl. 40). The presence of spots makes the computation of theoretical light-curves indeterminate. However, one may derive the effect produced by a bright equatorial zone (latitudes $< 30°$), assumed twice as bright as the polar regions; this has some resemblence to the brightness distribution found for I. With the same diameter as that used in computing Figure 23, *a*, the residuals for I are those shown in Figure 23, *c*. It is seen that the run of the residuals simulates one valid for a larger diameter but a uniform surface brightness which, of course, is not surprising.

9.3. Refraction and Absorption in Jupiter's Atmosphere

The effects of refraction and absorption on the observed light-curves of satellites as they go into eclipse have been considered by Link (1933) and others. In the simplest problem of this type the illumination is a point

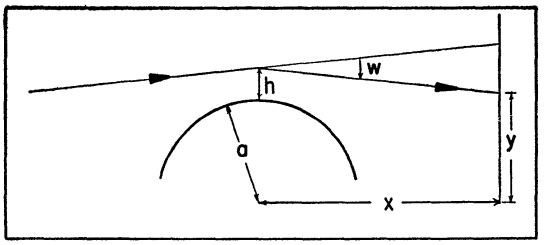

Fig. 24.—Schematic diagram of an occultation of a star by Jupiter

source at infinite distance, which applies to a stellar occultation by Jupiter. This case was considered earlier by Pannekoek (1903) and Fabry (1929). If the brightness of the star outside the occultation is taken as 100.0, the light-ray passing through the atmosphere will be refracted through an angle, w, and reduced to $B = 100/s$, where $s = 1 + wx/H$, if x is the distance of the observer from Jupiter and H is the scale height in Jupiter's atmosphere (Link, 1933, p. 245). This attenuation is caused by the light contained in a small solid angle being refracted into a larger solid angle; the attenuation due to absorption or scattering in the atmosphere is practically negligible by comparison.

If one imagines a screen set up at a distance x from Jupiter (Fig. 24), the intensity of illumination on the screen at a point y will be given by $B = 100/s$ and $y/H = \text{constant} - \ln(s - 1) - (s - 1)$ (cf. Link, 1933, p. 245). As the observer's motion on earth carries him across the screen, he will observe a light-curve, from which he can obtain the unknown, $1/H$.

The occultation of σ Arietis by Jupiter in 1952 was successfully observed by Baum and Code (1953) in the light of the K line of Ca II. From

their observed light-curve they concluded that $1/H$ lies between 0.08 and 0.16 km^{-1}; their adopted value of 0.12 leads to a mean molecular weight of 3.3, which is direct evidence for the predominance of H and He in the Jupiter stratosphere and is in agreement with Kuiper's (1952) model of the Jupiter atmosphere.

The formulae given for the attenuation of light assume that the angle of refraction is small. In the case of the occultation, this is an excellent approximation; for example, when $B = 1.0$ and hence $s = 1 + wx/H = 100$, $w = 0''.28$, x and H being known (see above). However, if one moves in to the distance of Jupiter IV, the same amount of refraction gives a brightness as high as $B = 77$. Similarly, the refraction which causes a star's brightness to decrease to 50 units reduces the brightness of Jupiter IV almost imperceptably to $B = 99.7$.

The effect of refraction on the satellites as they go into eclipse can be evaluated accurately if one assumes a model atmosphere for Jupiter; however, to a good approximation the results depend only on the scale height, H. It is necessary in the case of the eclipses to take the finite size of the sun into account, with allowance for limb darkening, and to perform the integration over the satellite's disk. This was done for the model atmosphere considered by Kuiper, which gives a scale height of 8.44 km, and applied to the case of Jupiter IV. Between $B = 100$ and $B = 0.2$ the resulting light-curve differs very little from the one computed by ignoring refraction; the small differences could easily be confused with residuals arising from a small error in the adopted satellite diameter. However, when refraction is allowed for, the light-curve of the eclipse does not terminate but decreases asymptotically to zero as $1/t$. In the case of Jupiter IV we find that, with no refraction, the brightness will be zero about 8 minutes after mid-eclipse; with allowance for refraction, the brightness at this time will be about $B = 0.2$ and 6 minutes later will be $B = 0.05$, corresponding to a total decrease of about 8.3 mag.

Because of the bright background, the limiting value of B that has been observed photoelectrically is approximately 0.2. However, visually the eye can follow the satellite to fainter limits: Kuiper (1947) has observed the satellites as they were eclipsed and noted a "halt" in the light-curves near fourteenth magnitude which lasts 1–2 minutes. It appears that his observations can be explained by the effects of refraction, as he had suggested. A summary of Dr. Kuiper's visual eclipse observations is given in Appendix III of this chapter.

Eropkin (1931), using a short-focus telescope, made photographic ob-

servations of the eclipses of Jupiter's satellites. These showed decreases in brightness, amounting to 30 or 40 per cent, several minutes before the predicted time of first contact, which led him and later Link (1933) to suggest the presence of an absorbing layer very high in Jupiter's atmosphere. This large pre-eclipse decrease is not present in the Harvard visual observations, in King's photographic observations, or in any of our photoelectric light-curves, though we made a special effort to discover any such peculiarity. Any such decrease could not exceed 0.2 per cent.

APPENDIX I

The exact solutions of the equations of radiative transfer for the problem of diffuse reflection are given by Chandrasekhar in his monograph, *Radiative Transfer* (Oxford, 1950), here denoted by "*R. T.*" These solutions are expressed in terms of numerical functions which have been tabulated for various values of the parameters. The following brief outline is an index to the formulae and tables of functions, used in the preparation of this chapter.

A. Planets with Optically Thick Atmospheres (Secs. 8.4–8.6 of This Chapter)

1. Isotropic scattering: Section 47 and Table XI in *R. T.;* D. L. Harris, *Ap. J.*, **136**, 408, 1957. More accurate values given by D. W. N. Stibbs and R. E. Weir, in *M.N.*, **119**, 512, 1959.
2. Anisotropic scattering: Section 47 and Tables XIX and XX in *R. T.;* D. L. Harris, *Ap. J.*, **136**, 408, 1957.
3. Rayleigh phase function: Section 47 and Table XXI in *R. T.*
4. Rayleigh scattering function: Section 70.3 and Table XXV in *R. T.*

B. Planets with Optically Thin Atmospheres (Sec. 8.8 of This Chapter)

1. Isotropic scattering: Section 72.2 in *R. T.* The allied functions are given by Chandrasekhar, Elbert, and Franklin, *Ap. J.*, **115**, 244, 1952, and Chandrasekhar and Elbert, *Ap. J.*, **115**, 269, 1952.
2. Anisotropic scattering: Section 72.2 in *R. T.* The necessary functions have not been evaluated.
3. Rayleigh phase function: Section 72.2 in *R. T.* The necessary functions have not been evaluated.
4. Rayleigh scattering function: Sections 72.3 and 72.4 in *R. T.* The allied functions are given by Chandrasekhar and Elbert, *Trans. Amer. Phil. Soc.*, Vol. **44**, Part 6, 1954.

APPENDIX II

Refraction Effects

The formulae quoted in Section 9.3 giving the effect of the Jovian atmospheric refraction on occultations of a star or on the light-curves of a satellite are based on Link's (1933) discussion. Consider a simplified model with the following characteristics:

1. Jupiter is a spherical planet with radius a, surrounded by an isothermal stratosphere with a scale height H.

2. The source of illumination, the sun or star, may be considered to be a point source located at a distance of $-X$ from Jupiter.

3. A screen is set up at a distance, $+x$, from Jupiter perpendicular to the line between the source and Jupiter.

In the absence of refraction a light-ray passing Jupiter at a radial distance of $a(1 + h)$ will strike the screen at a radial distance given by

$$y_0 = a\,(1+h)\left(1+\frac{x}{X}\right),$$

so that light-rays passing Jupiter at distances between $a(1 + h)$ and $a(1 + h + dh)$ will illuminate an annulus on the screen whose area is $dA_0 = 2\pi y_0 dy_0$.

Taking a total refraction, w, into consideration, the refracted ray will strike the screen at a radial distance given by

$$y = y_0 - wx\ ,$$

and the area of the illuminated annulus is $dA = 2\pi y dy$. It is convenient to transform out the effect of the distance of the source by letting $y_0' = y_0(1 + x/X)^{-1}$, and $x' = x(1 + x/X)^{-1}$. In the rest of the discussion we assume that this has been done and drop the superscript.

The brightness of the illuminated portion of the screen will be attenuated by $1/s$, where

$$s = \frac{y\,(dy/dh)}{y_0\,(dy_0/dh)} = \left(1-\frac{wx}{y_0}\right)\left[1-\frac{x\,(dw/dh)}{dy_0/dh}\right].$$

For the case where w = constant $\times\ e^{-ah/H}$ this reduces to

$$s = \left[1-\frac{wx}{a\,(1+h)}\right]\left(1+\frac{wx}{H}\right) \approx 1+\frac{wx}{H}.$$

Therefore, $(s - 1)H = wx$ = constant $\times\ x \times \exp(-ah/H)$, which gives ah/H = constant $- \ln(s - 1)$. Substituting in the equation for y, we obtain

$$\frac{y}{H} = \text{Constant} - \ln\,(s-1) - (s-1)$$

and

$$s = 1 + \frac{wx}{H}.$$

As noted in Section 9.3, the above formulae obtain in the case of an occultation to a high degree of approximation. For eclipses of Satellite IV the distance of the screen is only 0.0126 a.u. compared with 4.2 a.u. in the case of an occultation observed near opposition. For eclipses it is necessary to consider much larger refraction angles, as well as allow for the finite solar diameter, the solar limb darkening, and the finite disk of the satellite.

APPENDIX III

Visual Observations of Jupiter Satellite Eclipses

(Prepared by G. P. Kuiper)

Prior to the precision measures made photoelectrically, begun in 1950 and recorded in Dr. Harris' chapter, some visual observations of eclipses were made with the 82-inch telescope. These observations first called attention to the existence of a "tail" to each eclipse-curve near the fourteenth magnitude, which was tentatively attributed to refraction in the Jupiter atmosphere (Kuiper, 1947). Since the photoelectric data obtained so far do not go faint enough to bring out this tail clearly, the visual estimates are added here. The complete records are given as made at the telescope, although the estimates for the brighter portions have, of course, been entirely superseded by our photoelectric measures.

Jupiter I was observed on March 2, 1946. Mid-eclipse was predicted in the *Nautical Almanac* at $9^h49^m.0$ U.T.; corrected for the apparently constant ephemeris error of $-1^m.2$ (Table 32, above), the expected time was $9^h47^m.8$ U.T. The following are the observing records, made with power 660×:

9:47:47	about ½ disk left	9:50:01	about thirteenth magnitude
9:48:42	about ¼ disk left	9:50:07–22	near fourteenth magnitude
9:49:51	about eleventh magnitude	9:50:27	lost

The satellite stayed near the fourteenth magnitude for 10–15 seconds; only a crescent, not the entire disk, was visible (end of record). On the basis of the extrapolated light-curve of Figure 19, *a*, the satellite should have been lost about 9:50:05 U.T.; or, if 135 seconds were added to the predicted time of mid-eclipse (Sampson, 1907, p. 16), complete disappearance would have occurred at 9:50:03 U.T., 24 seconds before the satellite was actually lost.

Jupiter II was observed on March 2, 1946, also. Mid-eclipse was predicted for $11^h01^m.6$ U.T.; if the correction of Table 32 is applicable, the expected time is $11^h00^m.7$ U.T. The observing records are:

10:59:28	about $\frac{1}{2}$ disk left	11:02:33	about eleventh magnitude
11:00:33	about $\frac{1}{3}$ disk left	11:02:53	about twelfth magnitude
11:01:01	about $\frac{1}{4}$ disk left	11:03:03	about thirteenth magnitude
11:02:02	about ninth magnitude	11:04:18	lost

The limiting magnitude was estimated to be 14.5 mag. For a whole minute the satellite was around the fourteenth magnitude (end of record). With the half-duration of the partial phase 149 seconds (Sampson, 1907, p. 16), the predicted time of zero intensity is 11:03:11 U.T., 67 seconds before the satellite was actually lost.

Note added in proof.—DeVaucouleurs (1960) has reported some multicolor photometry of Mars, in which the stellar magnitude and integral albedo for Mars at five wave lengths (from 3300 to 6900 A) are derived on the basis of observations made at the Lowell Observatory in 1958.

REFERENCES

Ashbrook, J.	1948	*Pub. A.S.P.*, **60**, 116.
Barabashev, N. P., and Semejkin, B. E.	1933	*Zs. f. Ap.*, **7**, 290.
	1934	*Ibid.*, **8**, 179.
Baum, W. A., and Code, A. D.	1953	*A.J.*, **58**, 108.
Biesbroeck, G. van	1946	*A.J.*, **52**, 114.
Becker, W.	1928	*A.N.*, **235**, 85.
	1930	*Ibid.*, **239**, 19.
	1933	*Sitz. preuss. Akad. Wiss., phys.-math. Kl.*, **28**, 839.
	1948	*A.N.*, **277**, 65.
Bennett, A. L.	1938	*Ap. J.*, **88**, 1.
Bond, W. C.	1861	*Proc. Amer. Acad. Arts and Sci.*, N.S., **8**, 232.
Calder, W. A.	1936	*Harvard Bull.*, No. 903, p. 11.
	1938	*Ibid.*, No. 907, p. 26.
Campbell, L.	1917	*Harvard Circ.*, No. 200.
	1936	*Harvard Bull.*, No. 904, p. 32.
Chandrasekhar, S.	1950	*Radiative Transfer* (Oxford: Clarendon Press).
Danjon, A.	1933	*Ann. Obs. Strasbourg*, **2**, 170.
	1949	*Bull. Astr.*, **14**, 315.
	1954	*Ibid.*, **17**, 363.
Eropkin, D. J.	1931	*Zs. f. Ap.*, **3**, 163.
Fabry, C.	1929	*J. Observateurs*, **12**, 1.
Goddard, R.	1930	*A.J.*, **40**, 98.
Güssow, M.	1929	*A.N.*, **237**, 229.

GUTHNICK, P.	1918	*A.N.*, **206**, 157.
	1920	*Ibid.*, **212**, 39.
GUTHNICK, P., and PRAGER, R.	1918	*Veröff. Berlin-Babelsberg*, Vol. 2, Part 3.
HARDIE, R. H.	1953	*Lowell Obs. Progress Repts.*, No. 4.
	1956	Unpublished results.
HARDIE, R. H., and GICLAS, H. L.	1955	*Ap. J.*, **122**, 460.
HORAK, H. G.	1950	*Ap. J.*, **112**, 445.
HULST, H. C. VAN DE	1952	*The Atmospheres of the Earth and Planets* (rev. ed; Chicago: University of Chicago Press), chap. 2.
JOHNSON, H. L., and GARDINER, A. J.	1955	*Pub. A.S.P.*, **67**, 74.
JOHNSON, H. L., and MORGAN, W. W.	1951	*Ap. J.*, **114**, 522.
	1953	*Ibid.*, **117**, 313.
KEENAN, P. C., and MORGAN, W. W.	1952	*Astrophysics*, ed. J. A. HYNEK (New York: McGraw-Hill Book Co.), chap. I.
KING, E. S.	1917	*Harvard Ann.*, Vol. **80**, No. 10.
	1919	*Ibid.*, Vol. **81**, No. 4.
	1923	*Ibid.*, Vol. **85**, No. 4.
KUIPER, G. P.	1938	*Ap. J.*, **88**, 429.
	1944	*Ibid.*, **100**, 378.
	1947	*A.J.*, **52**, 147.
	1949	*Ap. J.*, **110**, 93.
	1952	*Atmospheres of the Earth and Planets* (rev. ed.; Chicago: University of Chicago Press), chap. 12.
	1953	*Proc. N.A.S.*, **39**, 1156.
	1956*a*	*J.R.A.S. Canada*, **50**, 170 ff.
	1956*b*	Unpublished.
LINK, M. F.	1933	*Bull. Astr.*, **9**, 227.
LOWELL, P., and SLIPHER, V. M.	1912	*Lowell Obs. Bull.*, No. 53.
MILFORD, N.	1950	*Ann. d'ap.*, **13**, 249, Table 2.
MINNAERT, M.	1941	*Ap. J.*, **93**, 403.
	1946	*B.A.N.*, No. 367.
MOORE, J. H., and MENZEL, D. H.	1928	*Pub. A.S.P.*, **40**, 234.
	1930	*Ibid.*, **42**, 330.
MORGAN, W. W., HARRIS, D. L., and JOHNSON, H. L.	1953	*Ap. J.*, **118**, 92.
MÜLLER, G.	1893	*Potsdam Pub.*, Vol. **8**, Part 4.
NIKONOVA, E. K.	1949	*Izvest. Crimean Astr. Obs.*, **4**, 114.
ÖPIK, E	1924	*Pub. Tartu (Dorpat)*, Vol. **26**, No. 1.
PANNEKOEK, A.	1903	*A.N.*, **164**, 5.

PICKERING, E. C.	1879	*Harvard Ann*., **11**, 266.
	1907	*Ibid.*, Vol. **52**, Part 1.
	1913	*Harvard Bull.*, No. 538.
RICHARDSON, R. S.	1955	*Pub. A.S.P.*, **67**, 355.
ROUGIER, G.	1933	*Ann. Obs. Strasbourg*, Vol. **2**, Part 3.
	1937	*Ibid.*, Vol. **3**, Part 5.
RUSSELL, H. N.	1916*a*	*Ap. J.*, **43**, 103.
	1916*b*	*Ibid.*, p. 173.
RUSSELL, H. N., DUGAN, R. S., and STEWART, J. Q.	1945	*Astronomy* (rev. ed.; Boston: Ginn & Co.), Appendix Table V.
SAMPSON, R. A.	1907	*Harvard Ann.*, **52**, Part 1.
	1909	*Ibid.*, Part 2.
	1910	*Tables of the Four Great Satellites of Jupiter* (London: W. Wesley & Son).
SCHÖNBERG, E.	1921	*Photometrische Untersuchungen über Jupiter und das Saturnsystem* (Helsinki: Finnish Academy of Science).
	1929	*Hdb. d. Ap.*, Vol. **2**, chap. 1.
SLAVINAS, P.	1928	*A.N.*, **233**, 125.
SHARONOV, V. V.	1939	*Pulkovo Circ.*, No. 27, p. 37.
	1940	*Ibid.*, No. 30, p. 48.
STEBBINS, J.	1927	*Lick Obs. Bull.*, No. 385.
STEBBINS, J., and JACOBSEN, T. S.	1928	*Lick Obs. Bull.*, No. 401.
STEBBINS, J., and KRON, G. E.	1956	*Ap. J.*, **123**, 440.
TALLEY, R. L., and HORAK, H. G.	1956	*Ap. J.*, **123**, 176.
VAUCOULEURS, G. DE	1960	*Multicolor Photometry of Mars in 1958*. (Scientific Rept. No. 3, ARDC Contract AF 19[604]-3074).
WALKER, M. F., and HARDIE, R. H.	1955	*Pub. A.S.P.*, **67**, 224.
WENDELL, O. C.	1913	*Harvard Ann.*, **69**, Part 2, 223.
WIDORN, TH.	1950	*Sitz. Öster. Akad. Wiss*, Ser. IIa, **159**, 189.
WOOLLEY, R. V.D.R.	1953	*M.N.*, **113**, 521.
WOOLLEY, R. V.D.R., and GASCOIGNE, S. C. B.	1948	*M.N.*, **108**, 491.
WOOLLEY, R. V.D.R., GOTTLIEB, R. K., and DE VAUCOULEURS, G.	1955	*M.N.*, **115**, 57.
ZÖLLNER, J. C. F.	1865	*Photometrische Untersuchungen* (Leipzig: W. Engelmann).